Università Campus Bio-Medico di Roma
School of Engineering
PhD Course in Biomedical Engineering

(XXI - 2005/2008)

A Technological Platform for Neurodevelopmental Studies

Fabrizio Taffoni

A Technological Platform for Neurodevelopmental Studies

A thesis presented by
Fabrizio Taffoni
in partial fulfillment of the requirements for the degree of
Doctor of Philosophy
in Biomedical Engineering
Universit`a Campus BioMedico
di Roma
School of Engineering

Coordinator
Prof. Saverio Cristina

Supervisor:
Prof. Eugenio Guglielmelli

Co-Supervisors:
Prof. Flavio Keller
Dr. Domenico Campolo

January 2009

Contents

Fabrizio Taffoni

List of Figures

List of Tables

Chapter 1

Introduction

Efforts converging in many different fields of research suggest that human movements are organized as *actions* and not *reactions*, that is, they are initiated by a motivated person, defined by a goal, and guided by information [1]. Several lines of research on normal motor development indicate that, even in a newborn, movements are not just reflexes, but have an intention [1, 2]. From birth onwards, children are involved in their world. When it comes to neurodevelopmental disorders with a genetic basis such as Autism Spectrum Disorder (ASD), Attention Deficit and Hyperactivity Disorder (ADHD), Tourette Syndrome, etc, behavioural analysis or phenotyping, is instrumental for the analysis of the roles of genes in behaviour [3]. Furthermore, brain circuits that have been traditionally considered to be involved in the regulation of motor output, such as the cerebellum or the basal ganglia, are now recognized to be also involved in non-motor functions, such as cognitive, mnemonic, and emotional functions [4, 5]. Taking all the above into consideration it is likely that behaviour disorder of neurodevelopmental origin usually diagnosed after language development, such as ASD, ADHD, Tourette Syndrome, and others, may be present as early as infancy.

Autism is a behavioural disorder, which begins in childhood, characterized by deficits in three basic domains: social interaction, language and communication, and pattern of interest. It is well known that autism has a strong genetic component, and that biological disease mechanisms leading to autism are already active during foetal development and/or infancy. This is demonstrated, for example, by abnormal pattern of brain growth during late foetal and early postnatal life (see [6] for a review). Autism is usually diagnosed at the age of 3 years and in many cases after a period of seemingly normal neurological and behavioural development. The diagnosis of autism is purely clinical as there are no laboratory tests to confirm or disprove the diagnosis. It has been recognized that, although typical autism is not associated with major neurological deficits, autism has characteristic manifestations in the perceptual and motor domains. Shortcomings in the perceptual domain include altered processing and recognition of socially relevant information from facial expression (see [7] for a review), deficits in perception of motion cues [8, 9, 10, 11], difficulty in disengaging attention [12] and alterations of auditory processing [13, 14]. Studies based on analysis of home-made movies suggest that an impairment of spontaneous attention toward social stimuli is present already at 20 months [15] if not sooner [16]. In addition, an autism-like syndrome is frequently observed in congenitally blind children [17]. All these observations suggest that at least some individuals with autism are characterized by an early deficit of "low-level" perceptual processing which jeopardizes their ability to develop higher-level capacities such as language and interpersonal skills. Motor impairments in autism include deficits in postural reflexes [18, 19, 20], repetitive, stereotyped movements and awkward patterns of object manipulation, lack of purposeful exploratory movements [21], gaze abnormalities [22] , unusual gait patterns [23], and alterations of movement planning and execution [24], which express themselves as "hyper-dexterity" [25, 26]. Motor abnormalities may be observed retrospectively in infants who later develop the autistic syndrome. This is based on home-made movies filmed during the first year of life [27, 28]. These clinical observations are consistent with a large body of evidence of subtle structural and functional abnormalities of cortical and subcortical neural systems involved in movement planning and execution, such as the prefrontal cortex, the basal ganglia and the cerebellum [6, 29, 30].

The diagnosis of ASD is currently made at the age of 3; ADHD is always considered as an alternative diagnosis of "high functioning" autism; Tourette Syndrome is diagnosed at age 7 or later.

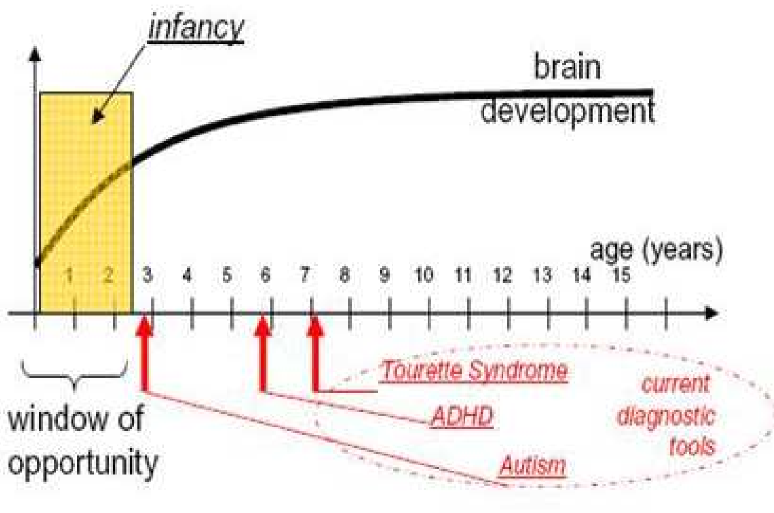

Figure 1.1: Current diagnostic tools

As shown in Fig.1.1, infancy, i.e. the first 2-3 years of life before language development, represents an important temporal window for an early diagnosis of ASD. Tests currently used for diagnosis are in the form of questionnaires [31] or consist in the observation of children's movements [28]. Goal-directed action in normally developing babies, can be assessed both under laboratory and naturalistic conditions. The most advanced technological set-ups available in research labs on autism/developmental disorders may currently include some sophisticated systems for movement analysis, such as:

- Stereophotogrammetric systems for movement analysis: these are rather sophisticated and costly technologies. They require highly structured environments. Generally cameras have to be carefully positioned and calibrated, leading to field-of-view problems, i.e. markers placed on the subject's body always have to be spotted by a given number of cameras in order to reconstruct their position in 3D space. Highly trained personnel are required to operate them;

- Gaze-tracking devices thus far in use, including commercially available ones, can be applied in specific contexts. Generally, the subject is required to face specific directions, e.g. they are particularly suitable when the subject looks at a TV monitor. Gaze tracking devices become unsuitable in the case of infants;

- Force platforms, often combined with photogrammetric systems, are used to measure Ground Reaction Forces (GRFs) as the subject walks on a platform. A major limitation is that measures are provided only when the subject steps onto the platform, i.e. they are not continual. Data extracted from a force platform are very useful when the walking pattern is somehow cyclic, i.e. the time the subjects stays on the platform is representative of the whole walking dynamics. In the case of infants and toddlers, clearly the time spent on the platform is no longer significant for the whole walking time;

- Data gloves: only recently some research projects are facing the problem of developing data gloves for children, which can be potentially combined with customized virtual reality environments.

A limitation common to all previously mentioned technologies is that, despite providing very accurate measurements, tasks need to be performed in well-controlled and highly structured environments as well as in accurately known and repeatable conditions. This is rarely possible when infants are involved and often impossible in poorly structured environments such as clinical cen-

Fabrizio Taffoni

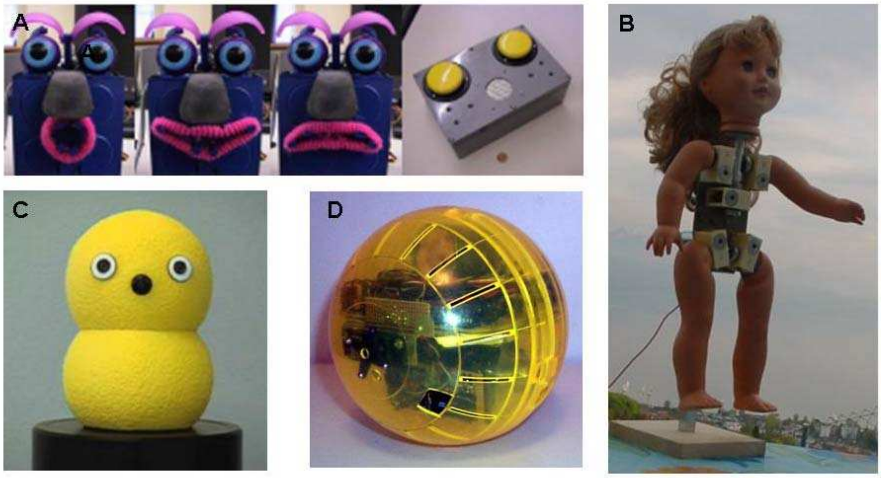

Figure 1.2: Robotic toys for therapy: *a)* three facial expressions from the ESRA robot and the Playtest device; *b)* Robota doll; *c)* Keepon robot; *d)* Roball

tres or nurseries. Deployment of state of the art technologies, e.g. interactive mobile robots, already proved potentially viable for research on autism [32].

Scassellati developed the ESRA robot (Fig.1.2.*a*), able to show a small set of facial expressions, with the aims of developing objective and quantitative methods and tools for autism diagnosis, of exploring the possibility of using robots as therapeutic aids, and of speculating on how the use of social robots in autism research might lead to a greater understanding of the disorder [33]. Dautenhahn and Billard [34, 35] used the Robota robot dolls (Fig.1.2.*b*), in the framework of the EU-funded AuRoRa Project to study if and how robots can have an educational or therapeutic role for children with autism. Robota is a 45 cm tall humanoid robotic doll. The Keepon robot (Fig.1.2.*c*) is a small puppet-like robot that conveys basic communicative actions, i.e. so-called attentive action and emotive action, which can be easily understood by children interacting with it. It has four motors, a rubber skin, two cameras in its eyes, and a microphone in its nose. In the context of Kozima's "Infanoid" project, Keepon studied the underlying mechanisms of social communication. Its simple appearance and behavior are intended

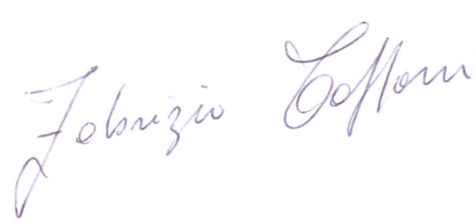

to help children to understand its attentive and emotive actions. The robot, usually under the control of a teleoperator, has interacted with children in schools and remedial centers for developmental disorders since 2003 [36]. The Roball (Fig.1.2.d) is a very simple robot in the shape of a ball, capable of intentional self-propelled movements and various interplay actions, by using motion, messages, sounds, illuminated parts, and other sensors. In trials with 2-to-4-year-old children it also proved to attract increased interest and engagement [37]. Another example of such kind of toys are the *Mental Commitment Robots* (MCR). MCR are developed to interact with human beings and to make them feel emotional attachment to the robots. Rather than using objective measures, these robots trigger more subjective evaluations, evoking psychological impressions such as "cuteness" and comfort. MCR are designed to provide 3 types of effects: psychological, such as relaxation and motivation, physiological, such as improvement in vital signs, and social effects such as instigating communication. These robotic toys have also been used with elderly people to prevent cognition disorders. It has also been demonstrated that it can contribute to improvements in long term care. An example of MCR is Paro, a therapeutic robot baby harp seal [38]. It has tactile sensors and responds to petting by moving its tail and opening and closing its eyes. It also responds to sounds and can learn a name. It can show emotions such as surprise, happiness and anger. It produces sounds similar to a real baby seal and (unlike a real baby seal) is active during the day and goes to sleep at night. However, mechatronic and ICT technologies have been used so far to provide new tools for therapy rather than for diagnosis. As a matter of fact, the only attempts at an early diagnosis of autism have been made by rating of home videotapes of behavior from very young children later diagnosed with autism [39]. This qualitative approach proved very useful in laying down the bases for research in this field but at the same time urges for novel quantitative approaches and enabling technologies.

Neuro-Developmental Engineering (NDE) is a new interdisciplinary research area at the intersection of developmental neuroscience and bioengineering aiming at providing new technologies and methods for: i) understanding neuro-biological mechanisms of human brain development; ii) quantitative analysis and modeling of human behavior during neuro-development; iii) assessment of developmental milestones achieved by humans from birth onwards. One of the most challenging applications of NDE is early detection of neuro-developmental disorders such as autism via a new generation of educational, interactive mechatronic toys that assess, guide, stimulate, and support the physiological neuro-developmental process [40, 41]. The goal of such approach is twofold. On one hand, guided by neuroscientists, developing technological platforms and methods to extract more information on perceptual and intersubjective capacities of human infants than is currently possible, this information could be later used for early diagnosis of developmental disorders. On the other hand, infancy provides us with an important window of opportunity to capture the mechanisms behind sensorimotor integration as these are just developing. Moreover, neurodevelopmental disorders are an important benchmark to highlight failures within such mechanism. Such a knowledge can be useful to neuroscientists to better understand the human brain functions involved in the sensorimotor integration but also to engineers, providing unique insights on how to build complex and adaptable artificial systems

Specifically, we propose the development of a new generation of educational, interactive toys that assess, guide, stimulate, and support the physiological neuro-developmental process. In particular, a new set of sensorized mechatronic toys is proposed. Such devices which could be considered the first example of a technological platform for NDE, have been specifically designed to measure user-toy interaction in non-structured environment focusing on children's motor behaviour [42, 43]. There are recent evidence in fact, which shows how brain and social skill development is strictly linked to the action: movements and cortical and sub-cortical areas shape each other

[44, 45]; understanding the meaning of an action or how to use an instrument seems to be possible thanks to the capability to replay that action or the use of that specific instrument. In particular the development of tool use ability seems to be a continuous process during which infants show a trial and error behavior which can be considered as self-generated opportunities for perceptual learning [46]. This platform is devised to extract more information on perceptual and intersubjective capacities of human infants than is currently possible; according to the goals of NDE this information is meant to be used for early diagnosis of neurodevelopmental disorders in infants. From a clinical viewpoint, the focus of our research work is on a specific disorder, that is autism. This choice helps us to identify clear functional and technical objectives for the technology we are developing. However, given the affinity of many neurodevelopmental disorders, e.g. in terms of their neural origin and behavioral manifestation, we foresee that results achieved on autism could be later generalized to the study and diagnosis of many other neurodevelopmental disorders, and vice versa.

Chapter 2

A technological platform for motor behaviour monitoring in infants and young children

As just said in the previous chapter, the few attempts at investigating the rationale for early diagnosis of autism have been made by *a posteriori* rating of home made videos of very young children's behavior [39]. This qualitative approach proved very useful in laying down the bases for research in this field but at the same time urges for novel quantitative approaches and enabling technologies. Based on this analysis, it can be stated that all technologies to be developed for the domain of Neuro-Developmental Engineering shall comply with strict functional and operative requirements, not fully met by current state-of-the-art. This work aims at developing conceptually new devices for neuro-developmental monitoring which respond to the following main requirements:

1. **Non-obtrusive technology**: the new devices shall be designed with the final goal of long-time monitoring but without being distressful to the child. In fact, the child should not perceive the presence of such instruments at all (e.g. wearable microphones, cameras, etc...), and

should like playing with them (e.g. instrumented toys). This clearly sets constraints on the kind of technology to be used. In particular, small size, light weight, wireless, and portable will be the key features to keep in mind during technical design of such devices.

2. **Minimally structured operating environments**: current tools for behavioral analysis, e.g. photogrammetric devices for motion analysis or force platforms for gait analysis or state-of-the-art gaze tracking devices, are not suitable for the screening of a large number of children for diagnostic purposes, mainly because of high costs and limited availability of the equipment. The development of relatively low-cost devices requiring minimally structured environments is proposed. Possible settings range from totally unstructured home-like situations, e.g. the child plays with interactive toys while a caregiver steers the game along predefined experimentally and diagnostically meaningful play protocols and tasks, to situations with an increasing degree of structuring.

It is worth underlining that these requirements, although desirable in every application involving systems for behavioral analysis, become strict constraints when the goals of NDE are addressed. In this respect, dealing with infants in ecological scenarios can be considered a real grand-challenge from the bioengineering viewpoint. Given the previous considerations, the main focus is conceiving and developing new integrated sensor technologies, having in mind two main typologies of applications relevant to the new domain of NDE:

- Wearable devices for movement analysis.

- Toys and objects of ordinary use in naturalistic scenarios, embedding miniaturized sensor and communication technology;

Whether wearable or embedded in regular toys, miniaturized technology for motion analysis is a key ingredient. In what follows, the development of integrated sensory modules which can be effectively integrated *in both* the typologies of technological platforms mentioned above is described.

Motion tracking can count on a a series of different technological solutions, operating on entirely different physical principles, with different performance characteristics and designed for different purposes. As shown in [47], there is not a single technology that can fit all needs. Each application defines the best technology to be implemented. In order to perform a selection, the main characteristics of available technologies are briefly summarized in what follows (see [47] for details):

- mechanical sensing: typically used for body motion capture; it uses angle and range measurements with the help of gears and bend sensors; very accurate but bulky, often limiting mobility;

- optical sensing: several principles are available, typical systems are camera-based ones; position of markers in 3D space can be estimated very accurately within working volume (typically a few cube meters, depending on the number of deployed cameras); line-of-sight issues (i.e. the fact that body parts or other objects may occlude the visual scene of a camera, thus losing the sight of one or more markers) is a limiting factor; very expensive; often requires highly structured environments, at least when high accuracy is needed;

- acoustic sensing: typically based on time-of-flight of ultrasound pulses between emitters and receivers; sound speed in air (about 340 m/s, resulting in sampling periods in the order of a few tens of milliseconds) is slow but still acceptable for sensing human (in particular infants) movements; line-of-sight issues are not as severe as for the optical technology; requires much less structured environments than optical trackers; suitable to be used in ecological conditions (e.g. kindergartens);

- (geo)magnetic sensing: a first method is based on electromagnetic coupling between a source and several trackers; main drawbacks are that signal decays as $1/d^3$ (where d is the source-tracker distance) and is affected by the geomagnetic field; these devices are quite expensive and require a certain amount of structuring of the environment; a second method is electronic compassing; estimates heading and solely relies on the geomagnetic field, i.e. it does not require any artificial source and is therefore sourceless; measurements can be altered by ferromagnetic influence of surrounding objects;

- inertial sensing: highly miniaturized accelerometers and gyroscopes are used to sense, respectively, acceleration (comprising the gravitational field) and angular velocity; used as inclinometers, accelerometers can sense the gravity vector, i.e. the "vertical" direction, in this sense they are also sourceless;

In Table 2.1, a selection chart for the different available technologies is provided. For each available technology (columns) its suitability with respect to the performance characteristics of interest (rows) is indicated. Since our main purpose is developing technological tools that are either wearable by infants or embeddable into toys, the highest priority is given to technologies which are unobtrusive. This directly leads us to discard solutions involving mechanical trackers.

The second element considered for selection is the line-of-sight issues, since we are going to deal with infants, it is extremely difficult to perform experiments with technologies that are limited by the line of sight, a peculiarity of the optical technology which is only suitable to experiments with collaborative subjects who are somehow willing to "act" in front of a camera. Line-of-sight issues are much less severe for the acoustic technology which is thus still appealing for movements analysis in infants.

The third element of the selection criterion is performance with respect to tracking accuracy. Here a distinction is made between tracking positions and tracking orientations. Measurement principles such as the time-of-flight (typically deployed in acoustic measurements) or camera-based tracking are inherently suitable to measure the distance of points (markers) and the origin

		Inertial	Geomagnetic	Acoustic	Optical	Mechanical
PRIORITY	tracker size / obstructive	+	+	+	+	--
	line-of-sight issues	+	+	+-	-	+
	tracking accuracy – orientation	+	+	-	+-	+
	tracking accuracy – position	-	-	+	+	+
	structured environment	+	+	+-	-	+
	working volume	+	+	-	-	-
	cost	+	+	+	--	-
SENSITIVE TO	ferromagnetic influence		-			
	acoustic noise			-		
	optical noise				-	
	temperature fluctuations	-	-	-		

LEGEND: + good; +- so and so; - bad; -- very bad

Table 2.1: Selection chart of different motion tracking technologies

of the measurement system (e.g. the source of acoustic waves or a camera etc...). Orientations can be inferred indirectly by estimating distances between two or more markers and the source of measurement. The larger the distance between two markers, the better the estimation of orientation. As dimensions shrink, as in the case of infants, accuracy of indirect orientation measurements also decreases (e.g. accurate tracking of the orientation of an infant's wrist can be problematic even without considering line-of-sight issues). Other technologies allow a direct measurement of orientations (for example inertial sensors used as inclinometers can sense deviations from the vertical axis while magnetic sensors used as compasses can sense deviations from the horizontal geomagnetic north direction) without requiring the positioning of multiple markers. So far, as long as orientation is concerned, inertial and magnetic technologies appear to be the most attractive since they: are highly unobtrusive due to the availability of miniaturized off-the-shelf devices; do not suffer from line-of-sight issues; can provide high accuracy in orientation tracking. Furthermore, relatively to any other alternative technology, inertial and magnetic technologies are sourceless and do not require any structuring of the environment, have virtually unlimited working volume and are available at very low cost.

The bottom half of Table 2.1 shows, for each technology, the main limiting factors to a correct operation. Besides temperature, which affects any electrical device and that can be compensated in most cases, the real limiting factor for the magnetic technology is the presence of ferromagnetic materials. Common ferromagnetic objects such as iron parts of doors, chairs, tables etc... can produce local distortions of the geomagnetic field, thus causing errors in the estimates of orientations. As discussed in [48], some care should be taken, when conducting experiments, to avoid large ferromagnetic objects in the surroundings. We found that this can be easily done in environments such as kindergartens where, for safety reasons, all metals are usually avoided and typical materials used with children are wood, rubber and plastic.

In what follows, the use of inertial/magnetic sensing for movement analysis will be described.

2.1 Measuring kinematics

Devices for measuring kinematics must not modify the infant's natural movement such as hand flapping, foot flapping, reaching to grasp movements, etc. A key element to satisfy such requirement is the *non-obtrusivity*. Non-obtrusivity is an age related concept: whath could be distressful for a newborn could not be for a one year old subject and vice-versa. For example the wired communication, which allows not to include the battery onboard and therefore to reduce the weight of the device, is not-obtrusive in infants since they are unable to turn their body but it becomes obtrusive in young children who are able to turn their body as well as to walk. For such reason a modular approach in designing sensorized toys for neurodevelopmental assessment in the first 2-3 years of life (Fig.1.1) has been followed. A core sensing unit which could be used both for wearable applications and sensorized smart toys, has been manufactured. In what follows such sensing unit, wired and wireless communication compatible, will be described.

Inertial and magnetic sensors provide measurements of *vector* quantities (e.g. accelerations, angular velocities and magnetic field) in a frame of coordinates relative to the sensor itself (moving frame). On the other hand, certain quantities are only known in a local frame of coordinates. For example, the gravity vector $\vec{g}$ can be expressed as $\vec{g} = [\ 0 \quad 0 \quad -g\ ]^T$ (where g = 9.81m/s^2) only in the local frame. Complementary filters and Kalman filters have traditionally been used to derive 3D orientation (attitude) from inertial and magnetic measurements. Fig.2.1 shows how to derive the orientation (represented as a rotation matrix R) of the moving frame with respect to the local frame using a complementary filter (see [49] for more details on the filter used).

Fabrizio Taffoni

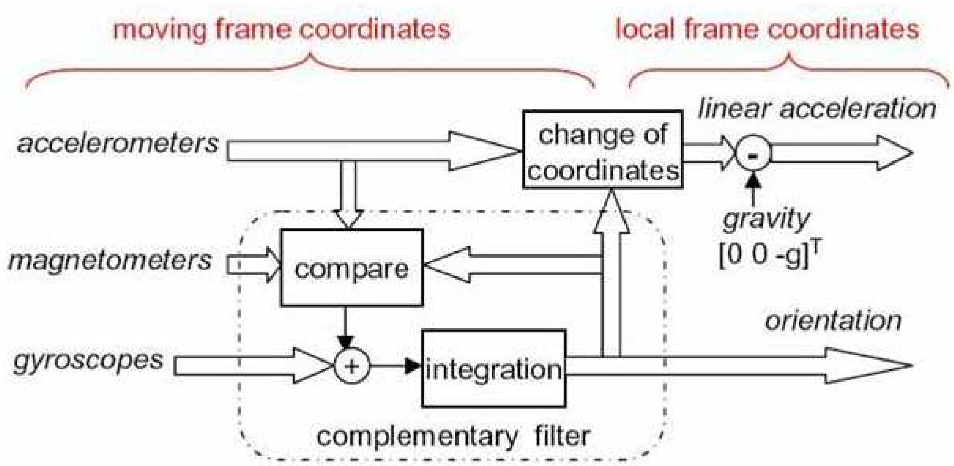

Figure 2.1:

Once the orientation matrix R is known, the components of the linear acceleration with respect to the local frame can be derived with a change of coordinates (via the same rotation matrix R) and by subtracting the gravity vector (whose components are known and constant in the local frame).

The full scale range of a sensor, given the full scale range of a set of available sensors, is selected as the minimum one containing the whole signal excursion. A smaller range may in fact lead to saturation when certain operative condition occurs, while a larger range would reduce sensitivity. In order to define technical specifications of the sensing unit, a preliminary quantitative analysis on main kinematical characteristics of spontaneous infants movements was carried out.

A three-camera (500 Hz) motion capture system was used (Qualysis Motion Capture Systems Inc., SWE) to obtain position-time data from both arms and hands of infants and evaluate frequency and dynamic content of their spontaneous movements. Three reflective non linear markers were

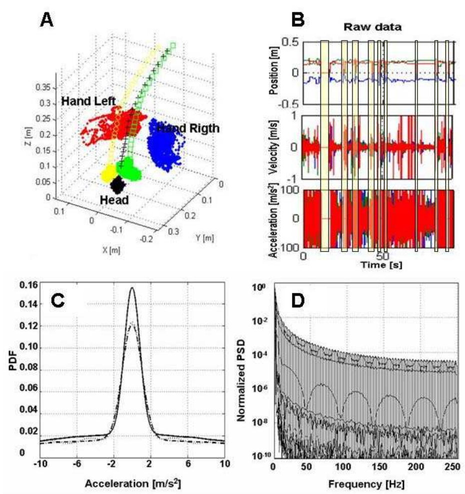

Figure 2.2: Preliminary kinematics analysis on one week old male infant: *a*) raw position data; *b*) acceleration and velocity reconstructed from raw position data; *c*) Probability Distribution Function (PDF) of the acceleration; *d*).Normalized Power Spectral Density (PSD)

placed on the head, respectively on the right, left and top head side, and two on the hands, right and left. In Fig.2.2.a, data on one week old male infant are shown. Accelerations with respect to a fixed reference frame were calculated from position data of wrist markers via a double time derivative (Fig.2.2.b). Velocity and acceleration are very noisy due to numerical estimation and spikes generated when the markers are out of sight (see yellow rectangles in Fig.2.2.b). Probability Density Function (PDF) has been calculated to split noise from signal in order to define the dynamic range for the accelerometer sensors (Fig.2.2.c). It shows that accelerations are included in the $\pm 2g$.

The Power Spectral Density (PSD) of normal infants'spontaneous movements has been also calculated. Raw position data have been segmented in vectors of 256 samples and the normalized short time Fourier transform has

	Accelerometers	Gyroscopes	Magnetometers
Range	$\pm 2g$	$\pm 1200/s$	$\pm$1Gauss
Bandwidth [Hz]	[0-50]	[0-50]	[0-50]
Sample frequency [Hz]	100	100	100

Table 2.2: Main requirements of magneto/inertial sensing unit

been calculated for each vector. Results in Fig.2.2.d show that movements can be considered band limited at 50 Hz: the power of the signal decreases of about 40 dB. This translates into an anti-aliasing filter cut-off frequency at 50Hz. A sampling frequency of 100 Hz has been considered to be the appropriate one, according to the Nyquist Theorem and in line with the most common sampling frequency used in movement analysis laboratory.

As for the magnetometers, since only the geomagnetic field (about 0.6 gauss) needs to be measured, the full measurement range should be in the order of 1 Gauss. Saturation of gyroscopes would result in a problematic loss of tracking and therefore, given several commercially available gyroscopes with full scale ranging from 150 deg/s to 1200 deg/s, the maximum scale range (1200 deg/s) was selected (see appendix for more details).

In summary, the magneto/inertial module should respond to these main requirements:

2.2 In-Field Calibration of Inertial/Magnetic Sensors

Magnetometers are meant to sense the geomagnetic field and provide its components $\begin{bmatrix} b_x & b_y & b_z \end{bmatrix}^T$ along the $\hat{x}$, $\hat{y}$ and $\hat{z}$ axes of the sensing device itself (such axes move with the moving frame). Similarly, the accelerometers are meant, in static conditions, to read out the components of the gravitational field $\begin{bmatrix} g_x & g_y & g_z \end{bmatrix}^T$ along the same axes. In fact sensors are just transducers and provide an output voltage V that, in the best scenario, is proportional to variations of the measurand m. In practical terms:

$$v = km + v_0 \tag{2.1}$$

where k and v_0 respectively represent the linear gain and the offset value. A calibration procedure is needed to determine such coefficients in order to derive the measurand m = $(v - v_0)/k$. Parameters v_0 and k are easily determined when situations exist where the measurand assumes (at least) two known values. In the case of accelerometers, the measurand can easily assume values 0, +g and −g by simply aligning (e.g. by means of mechanical set-ups such as a pendulum) the sensor's axis, respectively, orthogonal, parallel and anti-parallel with the vertical direction. Such a procedure, despite its apparent simplicity, can hardly be performed when the sensors are embedded into curvy toys (e.g. a ball), i.e. when the axes of the sensors cannot be aligned. When it comes to the magnetic field, alignment of the sensor axes with the field's direction is even more difficult. For this reason an additional field has to be generated. Commercially available devices such as the Honeywell HMC105X, a family of multi-axes magneto-resistive sensors, contain purposefully designed "offset straps", i.e. spirals of metallization that couple with each sensitive axis of the device producing an additional magnetic field. Such patented feature can be used for auto-calibration of the sensor. Such procedure requires addition of extra circuitry used to drive each offset strap with large currents, although for a very short time. In applications where infants are supposed to wear or use such technology, reduction of components is highly desirable. In [50], a procedure for in-field calibration of magnetometric sensors was presented which does not rely on previous knowledge of magnitude and direction of the geomagnetic field and which does not require accurately predefined orientation sequences. Such a method is especially useful in clinical applications since the clinician is no longer compelled to accurately execute complex calibration protocols. The procedure relies on the fact the geomagnetic field has constant components in the local frame. As the orientation of the sensors vary, the components in the moving frame also vary but are bound to lie on a particular ellipsoid, see [50] for details. Via the least-square method it is possible to estimate the centroid and semi-axes length of the ellipsoid which coincide with the calibration parameters. A calibration protocol was the set-up that would provide a number of measurements for the algorithm to robustly converge, as explained in the following. The instrumented toy (of whatever shape) is secured inside a wooden box, shaped as a parallelepiped, so that the toy would not move as the box is displaced around. The box is placed on a wooden table and it is used as a reference frame for the turning movements the calibration procedure is composed by. Three overall movement sequences are needed: one for each kind of sensor.

magnetometers: as in Figure 1-a, the box is placed on a table and an approximately 360 deg rotation (no need to be accurate) is performed by keeping one face of the box always parallel and in contact with the table. The same procedure is repeated for four different faces.

accelerometers: as in Figure 1-b, the box is placed on a table and smoothly (i.e. avoiding shocks) tilted by 90 deg along one edge, this is repeated four times[1] until the box returns in the initial position. The whole procedure is repeated with a different initial position.

Measurements derived from the calibration sequences are shown in Figures 2.3.a-c and 2.3.b-d, respectively for the magnetometers and for the accelerometers

The least-squares algorithm is then used to derive the best fitting ellipsoids (one for the magnetometers and one for the accelerometers) whose surfaces contain the two sets of measurements. As previously mentioned,

[1]Each time on a different edge: once a 90 deg rotation is performed along one edge, the next edge is the non-consecutive one which also makes contact with the table.

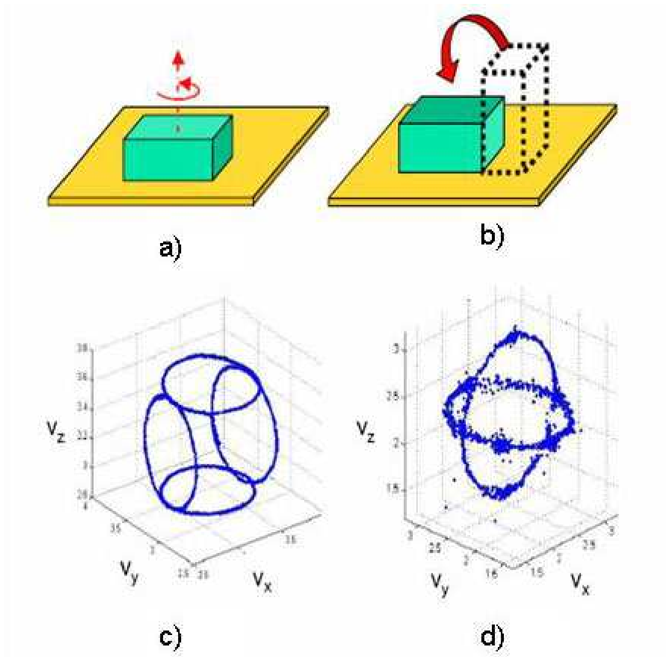

Figure 2.3: Calibration sequences for magnetometers (a) and accelerometers (b). Plots of the measurements (i.e. voltages Vx, Vy and Vz from the triaxial sensors) derived from the calibration sequences for the magnetometers (c) and the accelerometers (d).

since the geomagnetic field is constant, its components in the moving frame are bound to lie on the calibrating ellipsoid. This is so not only during the calibration sequences but for every possible movement. For this reason, also movements performed during the regular use of the toy, i.e. when the infant plays with it, can be used for updating the calibration parameters.

The offset values of gyros can be easily determined measuring their output in static condition i.e. without any rotation. To determine gains, three rotations about three *fixed* axes are performed. In what follows sensor axes are assumed to be perfectly orthogonal

A fixed reference frame has been defined using the gravitational and geomagnetic fields. Let $\{\mathbf{x}^0, \mathbf{y}^0, \mathbf{z}^0\}$ be the axes of the fixed reference frame with:

- $\mathbf{x^0}$: unitary vector pointing *East*
- $\mathbf{y^0}$: unitary vector pointing *North*
- $\mathbf{z^0}$: unitary vector pointing *Up*

These axes can be related to the the gravity vector **g** and geomagnetic field **b** as follows (see [50] for more details):

$$\mathbf{z^0} \triangleq -\mathbf{g}/g$$

$$\mathbf{x^0} \triangleq \mathbf{h}/ \parallel \mathbf{h} \parallel$$

$$\mathbf{y^0} \triangleq \mathbf{z^0} \times \mathbf{x^0} = \mathbf{h} \times \mathbf{g}/ \parallel \mathbf{h} \times \mathbf{g} \parallel$$

where **g** is is always vertical with respect to the earth surface; **h** is the vector defined by the cross product between **g** and the geomagnetic field $\mathbf{b}^2$. Let $\{\mathbf{x}^1, \mathbf{y}^1, \mathbf{z}^1\}$ be the axes of the mobile reference frame. To describe the orientation of the mobile reference frame with respect to the fixed reference frame an orientation matrix R_1^0 (from mobile to fixed reference frame) has been defined as:

$$R_1^0 \triangleq \begin{bmatrix} \mathbf{x^0} \cdot \mathbf{x^1} & \mathbf{x^0} \cdot \mathbf{y^1} & \mathbf{x^0} \cdot \mathbf{z^1} \\ \mathbf{y^0} \cdot \mathbf{x^1} & \mathbf{y^0} \cdot \mathbf{y^1} & \mathbf{y^0} \cdot \mathbf{z^1} \\ \mathbf{z^0} \cdot \mathbf{x^1} & \mathbf{z^0} \cdot \mathbf{y^1} & \mathbf{z^0} \cdot \mathbf{z^1} \end{bmatrix} \quad (2.2)$$

where " $\cdot$ " represents the Euclidean scalar product.

In order to be sure to keep constant the **v** axis (see 2.4), rotations of approximately $\pi/2$ rad are performed about one of the box sides. The orientation of the box with respect to the fixed reference frame before and after the movement can be defined respectively by the two rotation matrices $R_A^0$and R_B^0 (see Fig.2.4). The overall rotation about **v** axis is described by

[2] This vector points always towards East: geomagnetic field in fact is made by two components: an horizontal component $b_\parallel$ which points towards North and a vertical component $b_\perp$ so it does not contribute to the cross product.

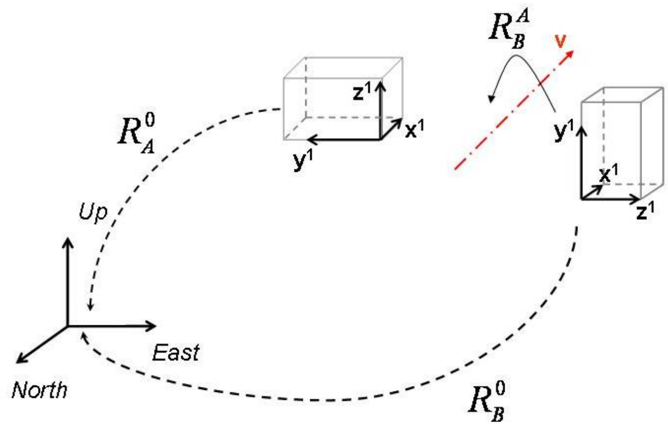

Figure 2.4: Fixed and moving coordinate frame during calibration of gyros

the following relationship:

$$R_B^A = (R_A^0)^T R_B^0 \tag{2.3}$$

Any orientation is equivalent to a rotation about a fixed axis $\mathbf{v}$ through an angle θ. The components of the vector $\theta\mathbf{v}\epsilon\mathbb{R}^3$ are called the *exponential coordinates* for R [51]. In particular for the R_A^B matrix these coordinates will be:

$$\theta\hat{\mathbf{v}} = log(R_A^B) \tag{2.4}$$

where $\hat{\mathbf{v}}$ is the skew symmetric matrix related to the unit vector axis $\mathbf{v}$ in the mobile reference frame and defined as:

$$\hat{\mathbf{v}} = \begin{bmatrix} 0 & -v_3 & v_2 \\ v_3 & 0 & -v_1 \\ -v_2 & v_1 & 0 \end{bmatrix} \tag{2.5}$$

In this case θ should be a scalar near the $\pi/2$ value (it depends by the angle between the two faces of the box which is not known *a priori*). Angular velocity vector can be therefore expressed as:

$$\boldsymbol{\omega}(\mathbf{t}) = \omega(t)\mathbf{v} = \omega_{\mathrm{x}}(\mathrm{t})\mathbf{i_x} + \omega_{\mathrm{y}}(\mathrm{t})\mathbf{i_y} + \omega_{\mathrm{z}}(\mathrm{t})\mathbf{i_z} \tag{2.6}$$

where i_x, i_y, and i_z are the unit vectors of the mobile reference frame. Knowing the exponential coordinates of rotation it is possible to write the following relationship:

$$\int\limits_T \boldsymbol{\omega}(\mathbf{t}) \cdot \mathbf{v}dt = \theta\mathbf{v} \tag{2.7}$$

where T is the time interval during which rotation is performed. Rewriting previous equation in terms of matrices, it becomes:

$$\int_T \begin{bmatrix} \omega(t)\mathbf{v}\cdot\mathbf{i_x} \\ \omega(t)\mathbf{v}\cdot\mathbf{i_y} \\ \omega(t)\mathbf{v}\cdot\mathbf{i_z} \end{bmatrix} dt = \theta \begin{bmatrix} \mathbf{v}\cdot\mathbf{i_x} \\ \mathbf{v}\cdot\mathbf{i_y} \\ \mathbf{v}\cdot\mathbf{i_z} \end{bmatrix} \tag{2.8}$$

where $\omega(t)\mathbf{v}\cdot\mathbf{i_x}$ is $\omega_x(t)$, $\omega(t)\mathbf{v}\cdot\mathbf{i_y}$ is $\omega_y(t)$ and $\omega(t)\mathbf{v}\cdot\mathbf{i_z}$ is $\omega_z(t)$. The three components of the rotation velocity are related to the voltage output of the sensor by the relation 2.1, that is the angular velocity about the general p axis is $\omega_p(t) = (V_p - O_p)/k_p$. Substituting this relation in the 2.8 it is possible to calculate the gain value k_p:

$$k_p = \frac{\int (V_p - O_p)dt}{\theta\mathbf{v}\mathbf{i_p}} \tag{2.9}$$

In particular, for numeric reason, among the relations in 2.8 the one which have the highest integral value[3] is chosen for each rotation.

[3] i.e. the sensor axis which is more parallel to the rotation axis: other axes will be an angular excursion near to zero.

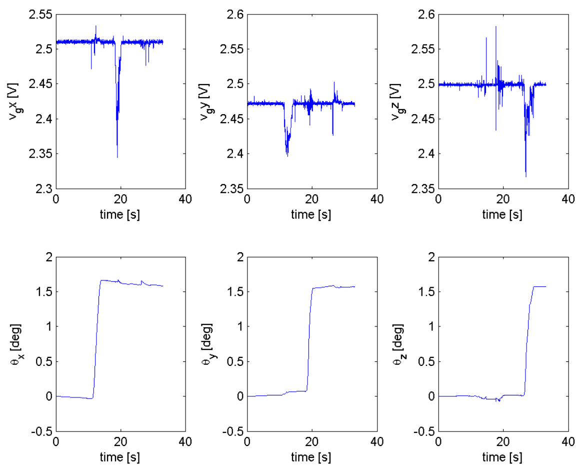

Figure 2.5: Plots of the measurements derived from the calibration of gyros

2.3 The Inertial/Magnetic Unit (IMU)

The first prototype of the IMU includes:

	Weight [g]	size [mm]	Range
two ADXL203 2-axes accelerometer	0.5	5x5x2	$\pm 1.7g$
three ADXRS300EB 1-axis rate gyro	0.5	7x7x3	$\pm 300°/s$
one HMC2003 3-axes magnetometer	2	26x19x11	$\pm$2Gauss

Table 2.3: Technical specifications of the first prototype

Devices were mounted as shown in Fig.2.6; in particular, attention was paid to guarantee that each sensitive axis was either orthogonal or parallel to the reference axes. Although size was not the main concern at this stage and no particular effort was paid towards miniaturization, the device could be easily embedded into a regular toy. Chosen devices provide a pre-amplified output, for this reason only anti-aliasing filtering was required before digitalization. Analog data provided by inertial/magnetic sensors and filtered by the anti-aliasing filter bank where acquired via two commercial A/D boards

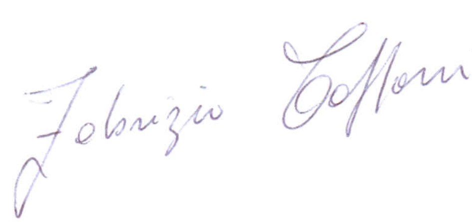

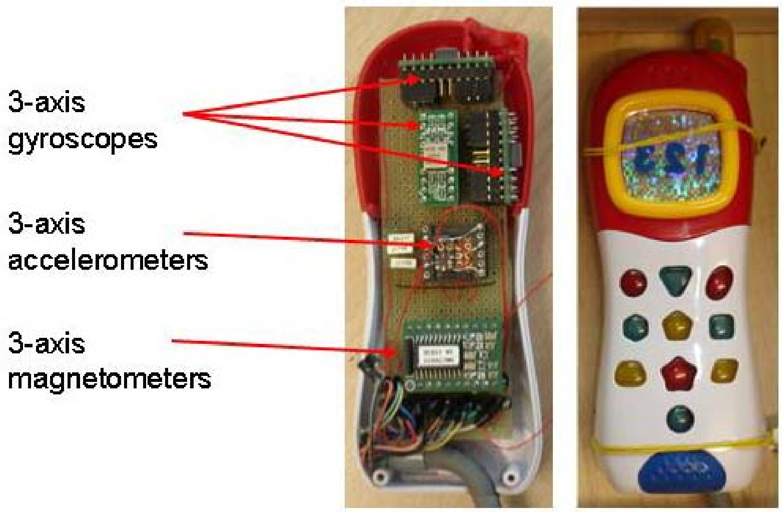

Figure 2.6: Inertial/magnetic sensing unit: first prototype embedded into a phone-like toy

(NI USB-6008, an 8 channels, 12 bits Analog to Digital acquisition board, National Instruments) which connected to PC via USB port.

The aim of the experimental work carried out was to provide a proof-of-concept of the proposed approach, i.e. to demonstrate the viability of the application of the proposed technology and calibration as well as processing techniques to this typical scenario. Two instrumented phone-like toys (each embedding 3-axis accelerometers, 3-axis gyroscopes and 3- axis magnetometers, similar to the one depicted in Fig.2.6 and calibrated via the procedure previously described) were used in a task where an educator and a 20 month old child were pretending to make a phone call, a camera with an internal microphone was also used to record the video-audio scene. The analog channels from the instrumented toys were acquired at 100Hz and stored on a PC for later analysis. Audio-video data from the camera were stored on tape and later transformed in a digital audio-video file. At the beginning of each ex-

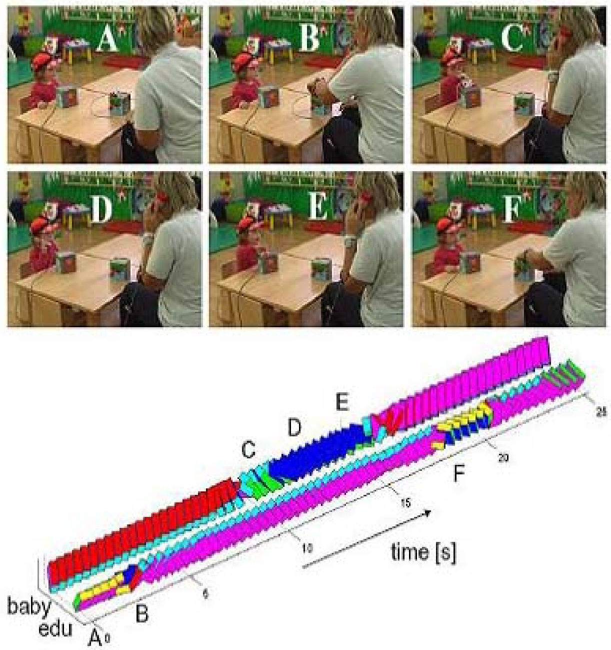

Figure 2.7: Sequence of images (A-F) from the experimental session (above). Plots of the orientations of the two instrumented toy-phones, one for the child (baby) and one for the educator (edu) versus time.

perimental session, a synchronization procedure has to be performed in order to be able to re-align, in a second time, audio, video and kinematic data for multimodal postprocessing. The synchronization procedure simply consists of banging the two toy-phones so that the same event can be recorded at the same time by the camera (whose internal microphone records the banging sound) and by each toy-phone (the shock produced during banging is detected by accelerometers embedded in each toy-phone).

As an example of use of tools embedding inertial/magnetic sensors, Fig.2.7 represents about 25 s of data extracted from an experimental session. After the synchronization procedure, the two toy-phones were placed in two boxes, one in front of the child and one in front of the educator (image A in Fig. 2.7). The educator starts the game (image B) by picking up her toy-phone and pretending to call the child, the child "answers" (image C) by picking up her toy-phone after a certain time (image D) and starts a "conversation". Then the child decides to "hang up" (image E) and the educator follows (image F). The bottom part of Fig.2.7 represents the evolution of the orientation of the two toy-phones with repect to time. The orientation was computed via the complementary filter in Fig.2.1.

These preliminary experimental results confirm the possibility to use such device in unstructured environments, i.e. ecological settings and, if necessary, in synchronous combination with other technologies (e.g. camera based tracking systems). Moreover such trials have highlighted the magneto/inertial technology is fully suitable to be used with infants allowing an automatic and objective data processing.

Although there are several highly miniaturized components available off the shelf, a microfabricated device integrating all the required sensing capability has been chosen for the final prototype of the inertial/magnetic sensing unit. There are two main reasons for such a choice: *(i)* a more efficient packaging; *(ii)* a more reliable axis orientation. Not orthogonal sensible axes directly translate in errors during orientation tracking.

A preliminary analysis of commercial magneto-inertial sensors at present available has highlighted a triaxial magnetometer, accelerometer and gyroscope analog sensor from Memsense (MAG02-1200S050) which matches technical requirements previously detailed (see Table 2.4)

	Acc	Gyro	Mag
Range	$\pm 2g$	$\pm 1200/s$	±1.9Gauss
Bandwidth [Hz]	50	50	50
Noise	$65\mu g/\sqrt{Hz}$	$50°/s/\sqrt{Hz}$	$60\mu V/\sqrt{Hz}$
MAG02-1200S050 size and weight			
Size [mm]	18x18x10		
Weight [g]	5		

Table 2.4: Technical specifications of MAG02-1200S050

Fabrizio Taffoni

MAG have an embedded anti aliasing filter at 50 Hz which matches technical requirements previously detailed. The 9 analog channels of the MAG are sent to an Analog to Digital Converter (ADC). ADC resolution was chosen keeping in mind electrical noise of the sensors embedded into the MAG, and angular resolution required. According to MAG datasheet, sensors are described as having the characteristics of white Gaussian noise. In particular accelerometer is the sensor with higher PSD. It is equal to 65 $\mu g/\sqrt{Hz}$ (table 2.4). After the low-pass (anti-aliasing) filter with bandwidth BW = 50Hz, the Root Mean Square (RMS) σ_g is given by:

$$\sigma_g = PSD\sqrt{1.6BW} \approx 0.58mg \tag{2.10}$$

where 1.6 is a correction term when a 1-pole low-pass filter is used. Considering a given sensitivity K_g = 1V/g, the output voltage RMS (σ_{gV}) is of about 0.58 mV. In static conditions, when an accelerometer is oriented so both its x-axis and y-axis are parallel to the earth's surface, it can be used as a 2-axis tilt sensor with a roll axis and a pitch axis. Once the output signal from the accelerometer has been converted to an acceleration that varies between −1 g and +1 g, the output tilt in degrees is calculated as follows:

$$\begin{aligned} Roll &= \arcsin(\tfrac{a_y}{g}) \\ Pitch &= \arcsin(\tfrac{a_x}{g}) \end{aligned} \tag{2.11}$$

Where a_x and a_y are, respectively, the accelerations along x and y-axis of the sensor. Let be n the number of bit resolution of ADC supplied at 5V. Then the Step Voltage (SV) readable from ADC in mV will be:

$$SV = \frac{10^3 \times 5}{2^n} \tag{2.12}$$

Therefore, taking the accelerometer readings at 0g (0° tilt for one axis) and

1g (90° tilt) the angular resolution will be:

$$
\begin{aligned}
RES(0) &= \arcsin(\tfrac{SV/K_g}{g}) \\
RES(90) &= 90 - \arcsin(\tfrac{g - SV/K_g}{g})
\end{aligned}
\tag{2.13}
$$

For a 12-bit ADC the SV will be about 1.2 mV (i.e less than 2) and angular resolution will be equal to 0.4° at 0° tilt and about 0.9° at 90° tilt in line with angular resolution of other commercially available magneto-inertial device (InterSense, Xsens, etc.). MAX1238 is a low-power, 12-channel, 12 bit AD Converters from Maxim-Dallas which fits the requirements detailed above. It has been chosen mainly for its serial I2C interface: each model of MAX1238 is uniquely identified by a 7 bit address which allows to exchange information coming from several modules (up to 4). After conversion, data are sent to a master station via I2C standard protocol. In this station a microcontroller PIC16F877A collects data from every MAX1238 (each identified by a unique address) and retransmits them via RS232 to a PC where they are stored.

The communication messages are built according to a standard structure: a message has two parts; one with a set of control communication fields (PREAMBLE, ID and CHECKSUM[4]) and one made by time stamps, sensors data bytes and battery voltage byte. Using this configuration the message has a total of 24 bytes. For a 100 Hz sampling frequency, the bit rate of the message will be equal to 24 kbps for each unit.

Preliminary tests carried out at Campus Bio Medico Kindergarten have highlighted the impossibility to use a wired connection with the remote master station in pretend play: children were distracted by the wire, it modifies their natural movements, it is unconfortable because children are able to walk, and it is potentially dangerous. Moreover the possibility to have a compact sensorized wireless object allows to study manipulation strategies while they are shaping. On the other hand, infants cannot walk yet and

[4]This byte should verify the integrity of the message. It is such that the sum of all bytes of the message is equal to zero.

Fabrizio Taffoni

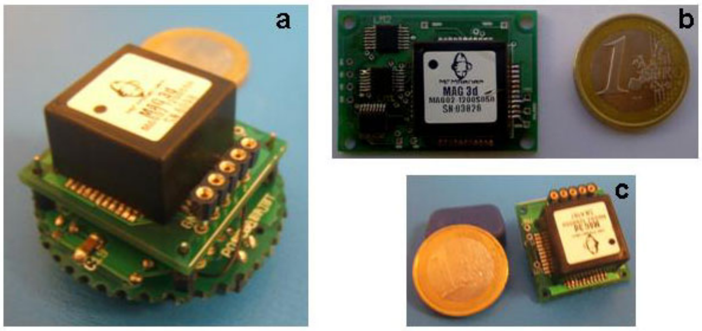

Figure 2.8: Kinematic sensing unit: *a)* wireless configuration *b)* wired configuration v1; *c)* wired configuration v2

they are not powerful enough to move sensor and battery together. For such reasons a wireless communication has been chosen for children while a wired communication has been chosen for infants. In the wirless IMU is tied together with the master station and batteries (Fig.2.8.a). Data are wireless transmitted from the master station to a PC where they are stored. In the wired configuration, IMU is connected by a 4 pole-wire (Serial CLock, Serial DAta, +5V and GND) to a *remote* master station where analog signals are digitalized and transmitted to a PC by a RS232 cable (Fig.2.8.b-c).

Among several wireless protocol available, the choice was restricted to the ones which allow an easy connection to a PC: mainly Wi-fi and BlueTooth (BT). Finally, BT was chosen for two main reasons: *(i)* BT protocol simplify the discovery and setup of services between devices; *(ii)* BT have a smaller power absorption than Wi-Fi. In particular, a class II BT transmitter was chosen: this allows a transmission range up to 10 m i.e. large enough for the specific application. According to such specifications a Parani ESD-200 from Sena Technologies, Inc. has been chosen. This module can be easily configured via AT commands and it has a compact design embedding on chip an antenna which allows a communication range up to 30 m.

Power consumption and supply are a key issue in every portable system. In order to choose the power source, energy consumption has to be esti-

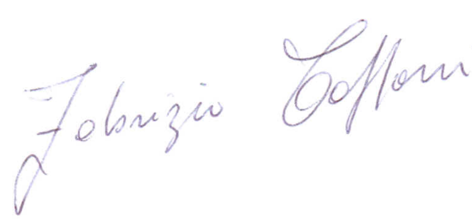

mated. Most of the energy is consumed by the Parani: it absorbs about 70 mA during transmission at 57600 bit/s. The only other power demanding component is the MAG sensor. Datasheets of MAG sensor report maximum 57 mA current (5V operating voltage). Other electronic components are very low power demanding. An over estimate of the total current is in the order of 150mA. To guarantee a continuous 1 hour operation, a minimum cell capacity C=150mAh is required. Usually, a larger capacity should be considered for two main reasons: *i)* in order to guarantee many life cycles (in case of rechargeable cells), a cell should never be discharged by more than 80% of its energy; *ii)* at high discharge rates the capacity falls steeply. As a "rule of thumb", a 1 hour discharge rate (i.e. fully discharging an xmAh cell at xmA) will reduce by half the available capacity, i.e. C´´=2C´. Considering rechargeable cells and according to previous considerations, the required capacity should be C''=2/0.8*150mAh=375mAh. The Li-Ion rechargeable batteries ENERGIZE SFE-1 made by Sony have been chosen mainly for their narrow dimension and weight. This battery has a capacity of 450mAh and provides 3.6V. Since MAG3 sensor requires 5V to operate while Parani 3.3V, at least a two-cells serial configuration is needed together with two voltage regulators.

The IMU itself has a total weight of about 8 grams and its size is about 24x24x20 mm. In wireless configuration the total weight of IMU, master board and battery is equal to 50 grams i.e. light enough to be manipulated by children.

Chapter 3

Applications of NDE technologies to motor behaviour analysis in toddlers and infants

In this chapter three applications of the presented technological platform are described and, where it is possible, data are discussed.

3.1 Objective assessment of *General Movements*

Infants show a large variety of *spontaneous movement* pattern. Such movements are called *spontaneous* to tell them apart from reflex movements. While reflexive movements allow to study in detail a stable, quantitative relationship between sensory input and reflexive motor output, spontaneous motility could be regarded as the expression of spontaneous neural activity, so it is an excellent marker of neural dysfunction caused by brain impairment.

General movements (GMs) are part of the spontaneous movement repertoire and they are present from early fetal life onwards until the end of the first six months of life.

GMs have been selected for the functional assessment of the young nervous system for three main reasons: *(i)* they are complex; *(ii)* they occur frequently; *(ii)* they are long enough to be observed properly. There are 4 main kinds of GMs (see [52] for more details):

1. **Writing Movements**: they are characterized by small to moderate amplitude and by slow to moderate speed. Typically, they are elliptical in shape, which creates the impression of a writing quality ;

2. **Fidgety Movements**: they are characterized by small amplitude, moderate speed, and variable acceleration of neck, trunk, and limbs in all directions continually in the awake infant except during fussing and crying;

3. **Cramped-Synchronized Movements**: they are characterized by rigidity and lack of the normal smoothness and fluency;

4. **Abnormal Fidgety Movements**: they are characterized by amplitude, speed, and jerkiness moderately or greatly exaggerated.

GMs in low-risk and high-risk infants or brain-damaged infants are not different with respect to the rate of their occurrence, i.e., their *quantity*, but they differ with respect to their *quality* [53], see Fig.3.1. The quality of GMs is probably modulated by corticospinal or reticulospinal pathways and, hence, can be affected by impairments of these structures. A disruption of the corticospinal projections by periventricular lesions of the corona radiata or internal capsule due to hemorrhages or hypoxic-ischemic lesions (leukomalacia) leads to abnormal GMs. GMs lose their complex and variable character and have either a poor repertoire, are cramped-synchronized, or chaotic. This definition holds true for the preterm and writhing GMs. Fidgety movements can be either abnormal or absent.

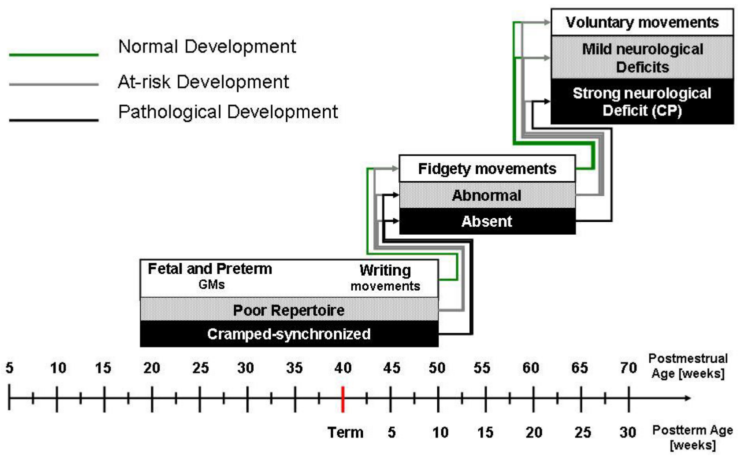

Figure 3.1: Adapted from [52] Development of GMs: a diagnostic tool for the functional assessment of the young nervous system

At the moment, the assessment of GMs is purely qualitative: infant, comfortably dressed (preferably with bare arms and legs), is videotaped in supine position for one hour, videos are then scored by trained personnel. In the *Perception in Action Laboratory* at Edinburgh University Qualysis Motion Capture System is being used to objectively assess GMs. The main drawback of this set-up is related to marker occlusion. In this work the use of the IMU is proposed to solve and improve respectively occlusion and portability issues of movement analysis systems like Qualysis and to automatically assess spontaneous infants'movements (see [56] for more details).

Since infants are not powerful enough to move large weight, the wired connection has been proposed in order to reduce the total weight moved by their hands and feet. According to anthropometric data [54] the device size should not exceed 3 cm in width and about 4-5 cm in length. Its weight should not exceed 20 g at all [55]. It should be provided with an easy and variable system, like Velcro straps, to fix it to the anatomical infant's segments. A first rigid structure of 40x30 mm has been designed and fabricated by a 3D fast prototyping printer from 3D ZCorporation, Inc. Such a mechanical solution

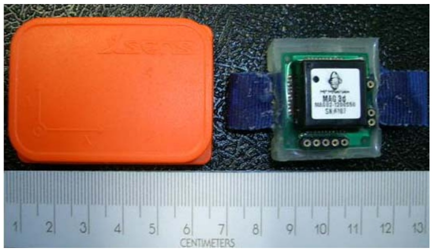

Figure 3.2: inserire figura x sens wams a confronto

was made by two parts: a support structure designed to bind up infant's limbs and a covering shell devoted to improve the infant's safety level and to avoid any possible contact between electric components and the infant's body. Although this structure fitted the mechanical constraints detailed above, a big problem was given by its weight and rigidness: the support structure alone, without covering shell and electric components, was 25 g in weight; the rigid material did not allow for a comfortable wearing by subject with different anatomical structures. For improving the anatomical adaptability and, at the same time, to reduce the total weight of the device, the structure has been realized by means of a silicon rubber material which does not need any mounting screws potentially dangerous for the child. The chosen rubber is the Silplay RTV 530 made by Prochima: it is an edible silicon used in the food industry. The structure has been realized in two steps: in the first one, rubber was dripped in a mold to form the flexible support structure; in the second one, the Velcro straps and electronic board were put into the mold on four square supports and a new rubber casting was made so that electronic and Velcro straps were embedded into the final structure. The total weight of the silicon support structure and electronic board is about 14g i.e. 30 grams lighter than state of the art magneto-inertial device commercially available and about 60% smaller.

When Optical motion capture systems are used to study limb movements of newborns, usually a fixed axis aligned to the head-foot direction is considered. The reason for this simplification is related to the fact that newborns usually tend to shake their limbs up and down along this direction[1]. According to such simplification a first test using IMU and Qualysis motion capture system has been executed. A marker has been placed on the magneto/inertial device and a common fixed reference frame has been defined for the two measurement systems. An up and down movement along one of the horizontal axes of the fixed reference frame (the y one) has been executed mimicking newborns' movements. Acceleration measured by the magneto/inertial sensor and the ones calculated by means of a double derivation of position data measured by Qualysis have been compared along y axis of the fixed reference frame. The mean error between the two traces is 0.0023 m/s^2 (about 0.23 mg) which is comparable with the electrical noise of the accelerometer sensors (see 2.10).

The second test performed was related to the possibility of reconstructing position and velocity data along the y-axis in case of marker occlusion. Velocity and acceleration can be calculated respectively as the first and second derivative of the position data. Let y[n], n ϵ[1,N] be the position data measured by Qualysis at frequency f_s and $\triangle T = f_s^{-1}$, the time interval between each sample. Velocity and acceleration calculated by position data are:

$$\begin{aligned} \dot{y}[i] &= \tfrac{y[i+1]-y[i]}{\triangle T},\ i\epsilon[1,N-1] \\ \ddot{y}[i] &= \tfrac{\dot{y}[j+1]-\dot{y}[j]}{\triangle T}\ i\epsilon[1,N-2] \end{aligned} \tag{3.1}$$

Supposing a marker occlusion between sample n_0 and n_0+K, velocity should be set to zero up to sample n_0+K where it should have a spike:

$$\dot{y}[n_0+K] = \frac{\dot{y}[n_0+K+1]-\dot{y}[n_0+K]}{\triangle T} \tag{3.2}$$

Theoretically, it is possible to reconstruct velocity and position data using acceleration a[n], nϵ[1,N] measured by a different measurement system by means of a double integration using suitable initial conditions. Unfortunately,

[1] The head-foot direction is the direction of feeding

using magneto-inertial technologies, acceleration signal (acc_{out}[n]) is affected by a low frequency noise $a_n[n]$:

$$acc_{out}[n] = a[n] + a_n[n] \tag{3.3}$$

When it is integrated, the estimated velocity in the interval [n_0-1,n_0+K] is:

$$\tilde{\dot{y}}[h] = \sum_{h=n_0}^{n_0+K} \frac{a[h]+a[h+1]}{2} \triangle T + \sum_{h=n_0}^{n_0+K} \frac{a_n[h]+a_n[h+1]}{2} \triangle T + \\ + \dot{y}[n_0-2] + \ddot{y}[n_0-2] \triangle T \tag{3.4}$$

where:

- $\sum_{h=n_0}^{n_0+K} \frac{a[h]+a[h+1]}{2} \triangle T$ is equal to the real velocity $\dot{y}$;
- $\sum_{h=n_0}^{n_0+K} \frac{a_n[h]+a_n[h+1]}{2} \triangle T$ is the drift error e[h] due to noise, i.e the difference between the real and the estimated velocity $e[h] = \tilde{\dot{y}}[h] - \dot{y}[h]$, h$\epsilon$[$n_0$, n_0+K];
- $\dot{y}[n_0-2] + \ddot{y}[n_0-2] \triangle T$ is the initial condition.

Assuming a linear drift function, i.e. a constant low frequency noise ($\frac{a_n[h]+a_n[h+1]}{2} = a_n, \forall h$), the drift error at sample n_0+K will be e[n_0+K]=K$a_n\Delta$T from which electrical low noise will be:

$$a_n = \frac{e[n_0+K]}{K \triangle T} \tag{3.5}$$

Knowing the real velocity at sample n_0+K+1, the drift error can be estimated as:

$$e[n_0+K] = \tilde{\dot{y}}[n_0+K] - (\dot{y}[n_0+K] - \ddot{y}[n_0+K] \triangle T) \tag{3.6}$$

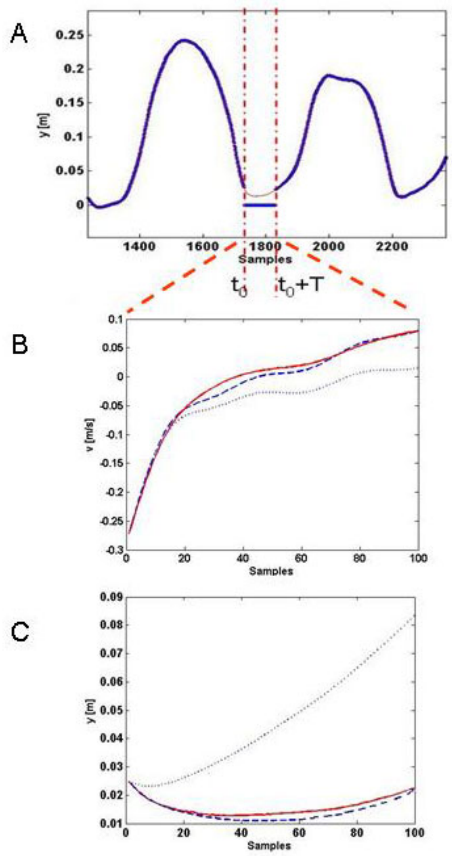

Figure 3.3: *a)* Simulated marker occlusion: red trace, real data; blue trace, simulated data;Velocity *(b)* and position *(c)* calculated from accelerometers data

Replacing e$[\mathrm{n}_0 + k]$ in3.5 with 3.6, it is possible to assess the electrical low frequency noise which can be used to adjust estimated velocity:

$$\hat{y}[h] = \tilde{y}[h] - (h - n_0)a_n \triangle T,\ h\epsilon[n_{0,}n_0 + K] \tag{3.7}$$

Where $\hat{y}[h]$ is the adjusted estimated velocity. A marker occlusion problem has been simulated filling a portion of position data with a sequence of 100 samples set to zero (3.3.A). In Fig3.3.B, velocity has been calculated from acceleration according to methodology discussed above: the red trace is the real velocity, the blue dotted trace is the estimated velocity with drift error and the dashed blue trace is the adjusted estimated velocity . The same process can be used to estimate position from $\dot{y}(t)$ (Fig.3.3.C).

3.2 Objective assessment of manipulation task

Goal-directed actions are guided by perceptual and cognitive processes and involve planning and anticipation. In particular, the ability to solve problems of how to relate objects to one another reflects infants' developing spatial perception and cognition. To fit an object into an aperture, for instance, infants must understand how the 2-dimensional aperture is related to the 3-dimensional object form and to plan the fitting action in a prospective and economical way which requires to imagine how to rotate the object in order to make it fit. These are rather sophisticated expressions of spatial cognition. They include mental rotation, as well as the ability to imagine goal states and understand means-end relationships. Thus, fitting tasks provide a window for learning about the development of these spatial abilities and how children go about solving them [57].

The IMU in the wireless configuration can be easily embedded into a set of bricks to study fine hand manipulation of infants involved in the block box game [58]. Such game is typically played by infants from 9 months of age. According to[57], the bricks set is made of a cube, a prism with a triangular cross section and a cylinder. The three different shapes allow us to study the fine orientation strategies in performing tasks with a different degree of difficulty; as well described in [57] the difficulty level of successfully completing the task depends on the number of different possibilities the children have to insert the brick into the right hole. In particular, they have no restriction in inserting the cylinder, eight different ways to insert the cube and only six ways for the prism with the triangular base. Moreover, the platform includes a base with holes fitting the shape of the bricks which allows to modify the relative orientation of the holes with respect to the infant's reference frame (Fig.3.4). Such feature of the base was specifically designed to monitor the capacity to redesign the environment [59]. To improve the likelihood of task success in fact, infants have only two possibilities: *(i)* changing the action repertoire used to perform the task (i.e. modify their movements *during* the

Fabrizio Taffoni

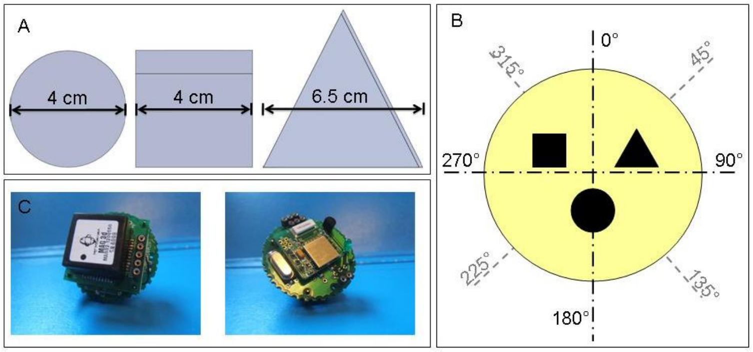

Figure 3.4: *(a)* Mechanical details ; *(b)* Moving base; *(c)* electronic core.

task) ; *(ii)* modifying the orientation of the holes and *then* performing the task.

A preliminary test has been performed with an adult subject in order to verify the possibility to measure differences in the motor strategies during insertion of the brick in the hole for different affordances. A prismatic and a cylindrical brick have been placed with their z axis horizontal with respect to global reference frame. In Fig.3.5 the roll, pitch and yaw angles are plotted. As can be seen from the graphs, the motor strategy used in order to insert the prismatic brick into the hole is more complex: it takes about 6.5 seconds and it needs three subsequent rotations to reach the goal. Instead, motor strategy used to insert the cylinder into the hole is simplest: it takes only about 2 seconds and it needs only one rotation to align the vertical axis of the shell to the vertical axes of the local fixed frame thanks to cylindrical symmetry.

3.3 Objective assessment of cerebellar functions

Movements can be defined in terms of coordination i.e. the cooperative interaction of many body parts and processes to produce a unified outcome. To assess the coordination skills, rapid execution of movements involving

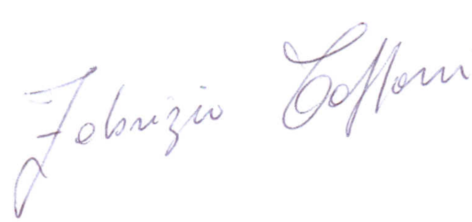

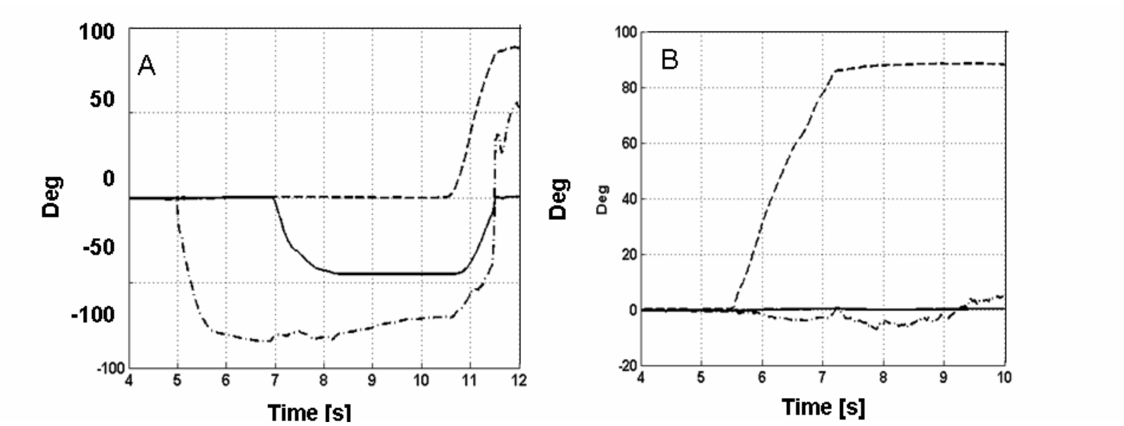

Figure 3.5: Orientation tracking: A) insertion of the prismatic shell B) insertion of the Cylindrical shell

alternate contractions of agonist and antagonist muscles is often used.

In 1902, Babinski coined the term *adiadochokinesis* to describe the inability to perform rapid pronation/supination of the hands in a patient suspected of having cerebellar dysfunction [60]. The diadochokinesis task is now used in many diagnostic tests to assess ataxia related to cerebellar dysfunction as well as effects of pharmacological treatment of neurological disorders e.g. Parkinson. Recent evidence has highlighted that also subjects with neurodevelopmental disorders, in particular High Functioning Autism (HFA) and Asperger Syndrome (AS), show strongest impairments executing such kind of movements. In particular, cerebellar abnormalities, with Purkinje neuron loss [30] and poor praxis performances as well as impaired diadochokinesis have been reported in Autism Spectrum Conditions (ASC) too [24, 61].

It is possible to assess diadochokinesis, coordination skills and motor processing abilities in typically developing children (CG) and children diagnosed with Autism Spectrum Condition (both HFA and AS), through the use of magneto-inertial devices applied to both wrists. Such kind of assessment is objective, unobtrusive and can be performed also in an unstructured environment provided that there are no ferro-magnetic objects or magnetic field source near the sensor (at least 1 meter).

The technology proposed was used in a pilot study on 31 consecutive subjects (15 ASC; 16 CG) aged 5-14 years matched for age, gender and IQ to evaluate the possible correlations between diagnosis, laterality, autistic traits and kinematic indexes. The kinematic performance, laterality and the number of autistic traits were assessed respectively by means of magneto/inertial sensors, Edinburgh Handedness Inventory test [62] and the children version of the Autism-spectrum Quotient (AQ-Child) [31], validated in Italian.

While children were engaged in a role game in which they were asked to perform the 12 actions listed in the Edinburgh handedness test, a clinician scored each one: +1 right hand/foot; -1 left hand/foot; 0 both. Parents were asked to fulfill the AQ-Child test for quantifying the number of autistic traits, in a continuum of severity, in all the subjects. The Total score (0-150) and the sub-scores in five different domains (Social Skills, Attention Switching, Attention to detail, Communication and Imagination) were rated.

After the laterality assessment, children, seated on a wooden chair in front of a table, were asked to perform 7 prono-supination trials. Kinematics of the movement were recorded by means of two magneto/inertial sensors. The two sensors (moving reference frames) were fastened to the wrists of the children in order to have the x axis parallel to the arm and the z axis going up. The two stylohyoid processes were used as repere points. A fixed global reference frame was defined to report each measurement (Fig. 3.6.A-B).

In the first trial children were asked to perform the prono-supination movement very accurately to assess their comfortable prono-supination velocity. In the second trial children were asked to perform the task at the maximum velocity they could in order to assess a sort of threshold of their performance. In the following five trials children were asked to move their limbs after a trigger acoustic stimulus at five different frequencies from 1 to 5 stimuli per second. A real time visual feedback (in form of a 3-D cube on a computer screen, representing the orientation of one wrist) was given to

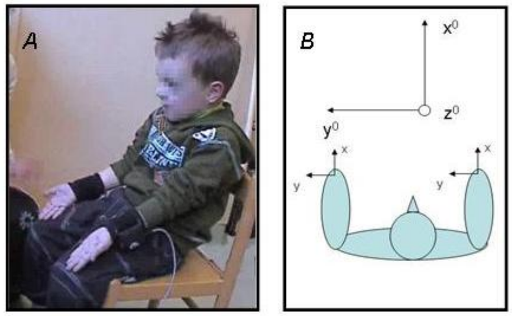

Figure 3.6: *a)* Child during the test; *b)* Magneto/Inertial reference frames

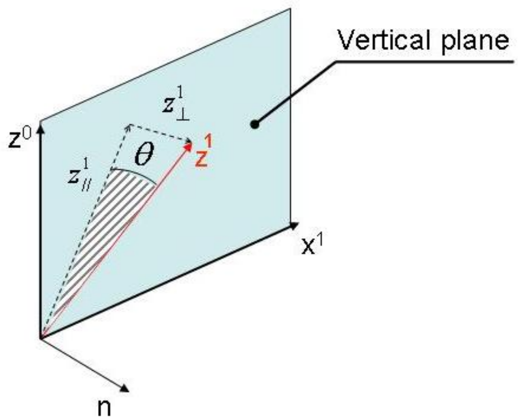

Figure 3.7: Definition of prono-supination angle

children in order to make the test more appealing.

The following motor variables and indexes were considered:

- **Prono-Supination Angle** $\vartheta(t)$: the *prono-supination angle* has been defined as the angle between the vertical plane (the plane between the fixed vertical axis z^0 and the moving axis x^1 whose normal vector n(t) is given by the cross product $n(t) = x^1(t) \times z^0$) and the z^1 moving vertical axis. According to the previous definitions and with reference to Fig. 3.7 the prono-supination angle can be defined as:

$$\sin(\vartheta(t)) = z^1(t) \cdot n(t) \tag{3.8}$$

$$z^1_\perp(t) = \sin(\vartheta(t))n(t)$$

$$z^1_\parallel(t) = z^1(t) - z^1_\parallel(t)$$

$$k(t) = unit(z^1_\parallel(t))sign(z^0 \cdot z^1(t))$$

$$\cos(\vartheta(t)) = z^1(t) \cdot k(t) \tag{3.9}$$

From 3.8 and 3.9 there follows the prono-supination angle:

$$\vartheta(t) = Atan2(\frac{\sin(\vartheta(t))}{\cos(\vartheta(t))}) \tag{3.10}$$

Where $z^1(t)=R(:,3,t)$ is the unit vector of moving reference frame at time t expressed in the fixed reference frame and $unit(z^1_\parallel(t)) = z^1_\parallel/\|z^1\|$;

- **Angular Velocity:** it has been computed from the rotation matrix according to the following relationship:

$$\hat{\omega}(t) = R(t)\dot{R}(t)^T, \hat{\omega}(t) = \begin{bmatrix} 0 & -\omega_{z0} & \omega_{y0} \\ \omega_{z0} & 0 & -\omega_{x0} \\ -\omega_{y0} & \omega_{x0} & 0 \end{bmatrix} \tag{3.11}$$

- **Linear Acceleration** ($\tilde{a}(t)$): it has been defined as:

$$\tilde{a}(t) = \vec{a}(t) - R^T\vec{g} \tag{3.12}$$

Where $a(\vec{t})$ is the acceleration measured by the inertial-magnetic sensor and $\vec{g}$ is the gravitational acceleration mapped on the moving reference frame by means of R^T.

- **Main Prono-Supination Axis:** It has been defined as the mean orientation of the axis around which the prono-supination movement takes place (see yellow axis in fig 3.8)

Fabrizio Taffoni

- **Prono-supination Frequency:** It has been defined as the inverse of the mean period of a complete prono-supination movements. The mean period T has been calculated using auto-correlation function of $\vartheta(t)$:

$$f_a(\tau) = \int_{-\infty}^{+\infty} \vartheta_s(t)\vartheta(t-\tau)dt \qquad (3.13)$$

  both for right and left side (s).

- **Inter-Axes Angle**: It has been defined as the angle between the two main prono-supination axes (left and right)

- **Prono-Supination Range:** It has been defined as the maximal angular excursion during the movement:

$$PSR = max(\vartheta(t)) - min(\vartheta(t)) \qquad (3.14)$$

- **Delay (d):** It has been defined as the value d at which the convolution function $f(\tau)$ is maximum:

$$f(\tau) = \int_{-\infty}^{+\infty} -\vartheta_r(t)\vartheta_l(t-\tau)dt$$

$$d : f(t = d) = max(f(\tau)) \qquad (3.15)$$

In figure 3.8 it is possible to see two typical plots of the kinematic data of a male control subject (Fig.3.8.A) and a male ASD subject (Fig.3.8.B). For each one, the prono-supination angle vs time according to (3.10) is plotted (upper part of the figure) as well as the orientation during the task, the angular velocity and the main prono-supination axis (bottom part of the figure). The two reference frames have the same origin O. In particular axes of the fixed reference frame, x^0,$y^0$and z^0, are represented by solid colored lines, respectively red, blue and green while axes of the mobile reference

Fabrizio Taffoni

frame, x^1, y^1, and z^1, by coloured dots, respectively red, blue and green: each dot marks the end of the axis at time t. The black dots are the normalized angular velocity: since movement is a pure rotation about a single axis, the distribution of these dots should be linear as it can be seen by the figure. The yellow axis represent the mean direction of the normalized angular velocity.

Preliminary data analysis showed:

1. No between-group statistical significant difference in the lateral preference (Table 3.1).

2. A statistically significant difference between ASC and CG in the AQ-Child total score and Social Skills, Attention Switching, Communication and Imagination sub-scores (Table 3.1).

3. A statistically significant difference between ASC and CG in the prono-supination frequency at 3 Hz (right). (Table 3.1)

4. A significant positive correlation between the Total AQ-Child and the prono-supination angle (right and left) at 2 Hz and the prono-supination frequency at 1 Hz, right and left, Table 3.2 (Fig.5 left).

5. A significant negative correlation between the Total AQ-Child and the prono-supination angle (left) at 5 Hz, Table 3.2 (Fig. 5B).

6. A significant positive correlation between AQ-Child Social Skills and the prono-supination angle (right and left) at 2 Hz and the prono-supination frequency at 1 Hz (right and left), Table 3.2.

7. A significant positive correlation between AQ-Child Attention Switching and the prono-supination frequency at 1 Hz (right and left), Table 3.2.

8. A significant negative correlation between AQ-Child Attention to detail and the prono-supination angle (left) at 5 Hz, Table 3.2.

Fabrizio Taffoni

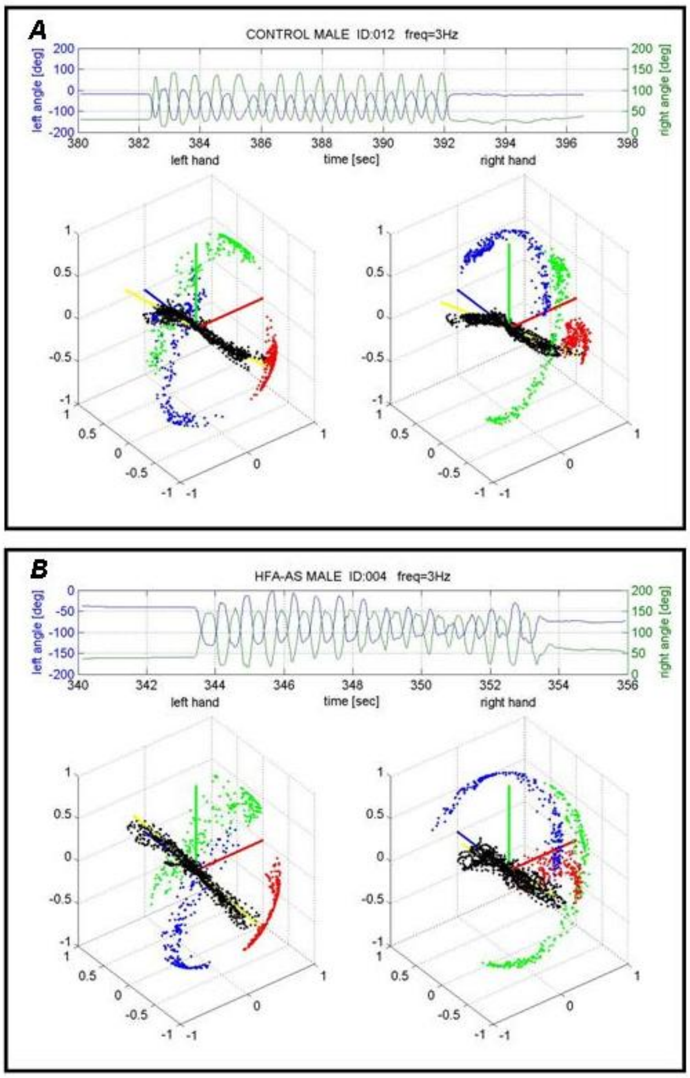

Figure 3.8: Prono-supination movements at 3Hz: A) control subject; B) HFA subject.

9. A significant positive correlation between AQ-Child Communication and the prono-supination frequency at 1 Hz (right). Table 3.2.
10. A significant negative correlation between AQ-Child Imagination and the prono-supination angle (left) at 5 Hz Table 3.2.
11. A significant positive correlation between AQ-Child Imagination and the prono-supination frequency at 1 Hz (right). Table 3.2.
12. A significant negative correlation between right-handedness and the inter-axes angle at 3 Hz, the prono-supination angle (left) at 5 Hz and the prono-supination frequency both right and left at 2-3 Hz. Table 3.3.

	Right-handedness	
	Pearson Correlation	Sig. (2-tailed)
Inter-axes angle at 3 Hz	-0.39	0.03
Prono-supination angle Left-5 Hz	-0.39	0.03
Prono-supination freq. Right-2 Hz	-0.45	0.01
Prono-supination freq. Left-2 Hz	-0.45	0.01
Prono-supination freq. Right-3 Hz	-0.39	0.04
Prono-supination freq. Left-3 Hz	-0.40	0.03

Table 3.3: Statistically significant correlations – Handedness

Fabrizio Taffoni

	Group	**Mean**	**SD**	**t-test (df=29)**	**Sig. (2-tailed)**
Edinburgh Handedness Inventory	ASC	0.67	0.53	0.461	0.648
	CG	0.58	0.54		
AQ total (child)	ASC	90.1	17.72	5.753	0.000***
	CG	49.6	21.19		
AQ social skill	ASC	18.7	6.65	4.881	0.000***
	CG	8.6	4.87		
AQ attention switching	ASC	18.3	5.35	4.553	0.000***
	CG	9.3	5.58		
AQ attention to detail	ASC	16.7	4.86	0.979	0.335
	CG	14.4	7.74		
AQ communication	ASC	20.1	4.39	7.489	0.000***
	CG	8.4	4.3		
AQ imagination	ASC	16.3	5.19	4.431	0.000***
	CG	8.9	4.06		
Prono-Supination frequency	ASC	1.43	0.05	-2.1	0.048*
	CG	1.5	0.12		

Table 3.1: Mean, SD and t-test between ASC and CG – statistical significant contrasts (* $p<0.05$; *** $p<0.001$)

	AQ-Child Total	
	Pearson Correlation	Sig. (2-tailed)
Prono-supination angle Right-2Hz	+0.38	0.03
Prono-supination angle Left-2Hz	+0.40	0.02
Prono-supination freq. Right-1 Hz	+0.48	0.008
Prono-supination freq. Left-1 Hz	+0.38	0.04
Prono-supination angle Left-5 Hz	-0.42	0.02
	AQ-Child Social Skills	
	Pearson Correlation	Sig. (2-tailed)
Prono-supination angle Right-2 Hz	+0.42	0.02
Prono-supination angle Left-2 Hz	+0.43	0.01
Prono-supination freq. Right-1 Hz	+0.52	0.0004
Prono-supination freq. Left-1 Hz	+0.45	0.01
	AQ-Child Attention Switching	
	Pearson Correlation	Sig. (2-tailed)
Prono-supination freq. Right-1 Hz	+0.50	0.006
Prono-supination freq. Left-1 Hz	+0.42	0.02

	AQ-Child Attention to detail	
	Pearson Correlation	Sig. (2-tailed)
Prono-supination angle Left-5 Hz	-0.41	0.02
	AQ-Child Communication	
	Pearson Correlation	Sig. (2-tailed)
Prono-supination freq. Right-1 Hz	+0.37	0.048
	AQ-Child Imagination	
Prono-supination angle Left-5 Hz	-0.39	0.03
Prono-supination frequency Right-1 Hz	0.45	0.01

Table 3.2: Statistically significant correlations – AQ-Child

From preliminary data analysis it seems that the presence of autistic traits, detected through the AQ-Child, are related to the different kinematic indexes according to a bimodal pattern that is associated to the frequency of prono-supination: At lower frequencies, which are very close to the comfortable one, it seems that the more autistic traits you display the better you perform; at higher frequency (5Hz) the pattern seems to become the opposite – i.e. the more autistic traits you show, the worse you perform. Further more complex analyses are needed to confirm these early preliminary results and other research is warranted to better clarify the potentially peculiar patterns of motor impairment and dyspraxia in ASC. However these findings seem to be in agreement with the hypothesis of cerebellum as an interval timing system [63, 64, 65], deputed to assess millisecond time intervals. The reduced number of Purkinje cells modifies the inhibitory cortical side loop in

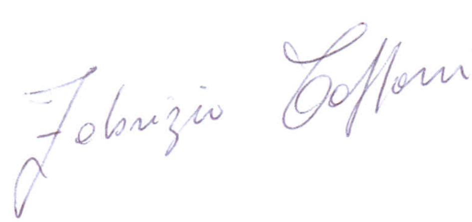

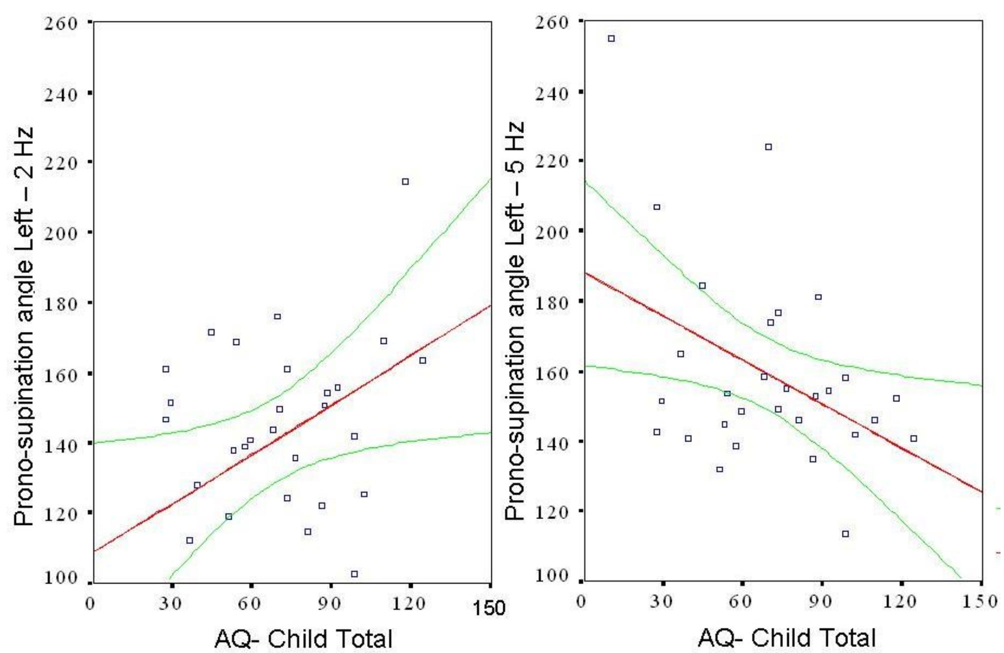

Figure 3.9: AQ-Child Tot/ Prono-supination angle Left-2 Hz and Prono-supination angle Left-5Hz

the cerebellar control system. Such alterations could affect the possibility to discriminate the millisecond time intervals observed in ASC subject at higher frequency, that is the ones which require a higher cerebellar control.

Chapter 4

Conclusion

In this work, a novel technological approach called Neuro-Developmental Engineering is presented. Its main objective is to provide neuroscientists with novel technological platforms for the unobtrusive and ecological assessment of behavioral development in infants; these may lead to novel, quantitative, objective, and cost-effective tools for detecting early signs of neurodevelopmental disorders.

A set of sensorized devices for human motor behaviour and neurodevelopmental milestone assessment has been designed: wearable devices and smart toys. For all these devices, the design criteria take primarily into account the final use: monitoring *natural movement* of a large number of babies in a *natural environment*. For this reason, such devices have been designed to operate in minimally structured environments, in ecological scenarios, as standalone or in conjunction with other devices. In fact, we strongly believe that early diagnosis of neurodevelopmental disorders will be made possible not just by a single, perhaps sophisticated, device but by a multimodal assessment of different perceptual and motor domains. On the other hand, low-cost technology is crucial for devices that are meant for early diagnosis: screening of a large number of infants would not be possible with costly technology. After a technological state of the art review, magneto/inertial sensors have been chosen. The design of an electronic core which could be either wearable by 6 month old babies, or be embedded in toys like balls or cubes has been carried out. A simple calibration procedure based on rotation movements has been set up. Such procedure can be performed in an unstructured environment (ranging from fully unstructured home-like situations to more structured situations such as Neonatal Intensive Care Units) and by untrained personell.

Three applications are described, and data, where present, discussed: wearable sensors for measuring spontaneous movements (upper and lower limbs) in premature babies; an instrumented toy for assessment of manipulation skills in infants from six months onward; a wearable magneto/inertial module for objective assessment of motor impairments with focus on diadocockinetic movements in children.

The first few prototypes have recently been released to 4 children's clinical centres in Europe and the challenge will be the interpretation of data recorded in ecological scenarios with the aim of detecting potential abnormalities in development.

Appendix A

Electronic Design: part list and schematic

Exported from *IMU.sch* at 30/01/2009 12.34.12

EAGLE Version 4.16r2 Copyright (c) 1988-2006 CadSoft

Part	**Value**	**Device**	**Package**	**Library**	**Sheet**
C1	15pF	C-EUC1206	C1206	rcl	1
C2	15pF	C-EUC1206	C1206	rcl	1
C3	15pF	C-EUC1206	C1206	rcl	1
C4	15pF	C-EUC1206	C1206	rcl	1
C5	15pF	C-EUC1206	C1206	rcl	1
C6	15pF	C-EUC1206	C1206	rcl	1
C7	0.1uF	C-EUC1206	C1206	rcl	1
C8	100uF	C-EUC1206	C1206	rcl	1
C9	0.1uF	C-EUC1206	C1206	rcl	1
C10	0.1uF	C-EUC1206	C1206	rcl	1
C11	0.1uF	C-EUC1206	C1206	rcl	1
C12	0.1uF	C-EUC1206	C1206	rcl	1
C13	0.1uF	C-EUC1206	C1206	rcl	1

Part	Value	Device	Package	Library	Sheet
C14	0.1uF	C-EUC1206	C1206	rcl	1
C15	0.1uF	C-EUC1206	C1206	rcl	1
C16	4.7uF	CPOL-EUE2,5-6E	E2,5-6E	rcl	1
C17	0.1uF	C-EUC1206	C1206	rcl	1
C18	10uF	C-EUC1206	C1206	rcl	1
C19	0.1uF	C-EUC1206	C1206	rcl	1
C20	100uF	C-EUC1206	C1206	rcl	1
C21	16pF	C-EUC1206	C1206	rcl	1
C22	16pF	C-EUC1206	C1206	rcl	1
C23	100uF	C-EUC1206	C1206	rcl	1
IC2	TC-1262-3.3	LM340MP-05	SOT223	linear	1
IC3	LM2931	78L05Z	TO92	linear	1
IC4	PIC16F876SO	PIC16F876SO	SO28W	microchip	1
IC5	7805T	7805T	TO220H	linear	1
LED1		LED3MM	LED3MM	led	1
MAG_1	MAG_02	MAG_02	MAG_02	custom	1
MAX1	MAX1238	MAX1238	QSOP16	custom	1
Q1	20MHz	CRYSTALSM49	SM49	crystal	1
Q2	20 MHz	CRYSTALSM49	SM49	crystal	1
Q3	20 MHz	CRYTALSM49	SM49	crystal	1
Q4	20 MHZ	CRYSTALSM49	SM49	crystal	1
R1	47K	R-EU_R1206	R1206	rcl	1
R2	47K	R-EU_R1206	R1206	rcl	1
R3	47K	R-EU_R1206	R1206	rcl	1
R4	330R	R-EU_R1206	R1206	rcl	1
R5	470k	R-EU_R1206	R1206	rcl	1
R6	470k	R-EU_R1206	R1206	rcl	1
R7	47k	R-EU_R1206	R1206	rcl	1

Fabrizio Taffoni

Part	**Value**	**Device**	**Package**	**Library**	**Sheet**
R8	120k	R-EU_R1206	R1206	rcl	1
R9	68k	R-EU_R1206	R1206	rcl	1
R10	2.2k	R-EU_R1206	R1206	rcl	1
R11	2.2k	R-EU_R1206	R1206	rcl	1
R12	2.2k	R-EU_R1206	R1206	rcl	1
R13	2.2k	R-EU_R1206	R1206	rcl	1
R14	2.2k	R-EU_R1206	R1206	rcl	1
R15	2.2k	R-EU_R1206	R1206	rcl	1
U$1		LED3MM	LED3MM	led	1
U$12	PROMI2	PROMI2	PROMI2	custom	1
U$13	MAX232_TI		SO16	custom	1
U1		PIC16F876	SO-28W	pic16f87x	1
U2		PIC16F876	SO-28W	pic16f87x	1
U3		PIC16F876	SO-28W	pic16f87x	1
X1		FSIDE-6	FSIDE-6	con-amp	1
X2		FSIDE-6	FSIDE-6	con-amp	1
X3		FSIDE-6	FSIDE-6	con-amp	1
X4		FSIDE-6	FSIDE-6	con-amp	1

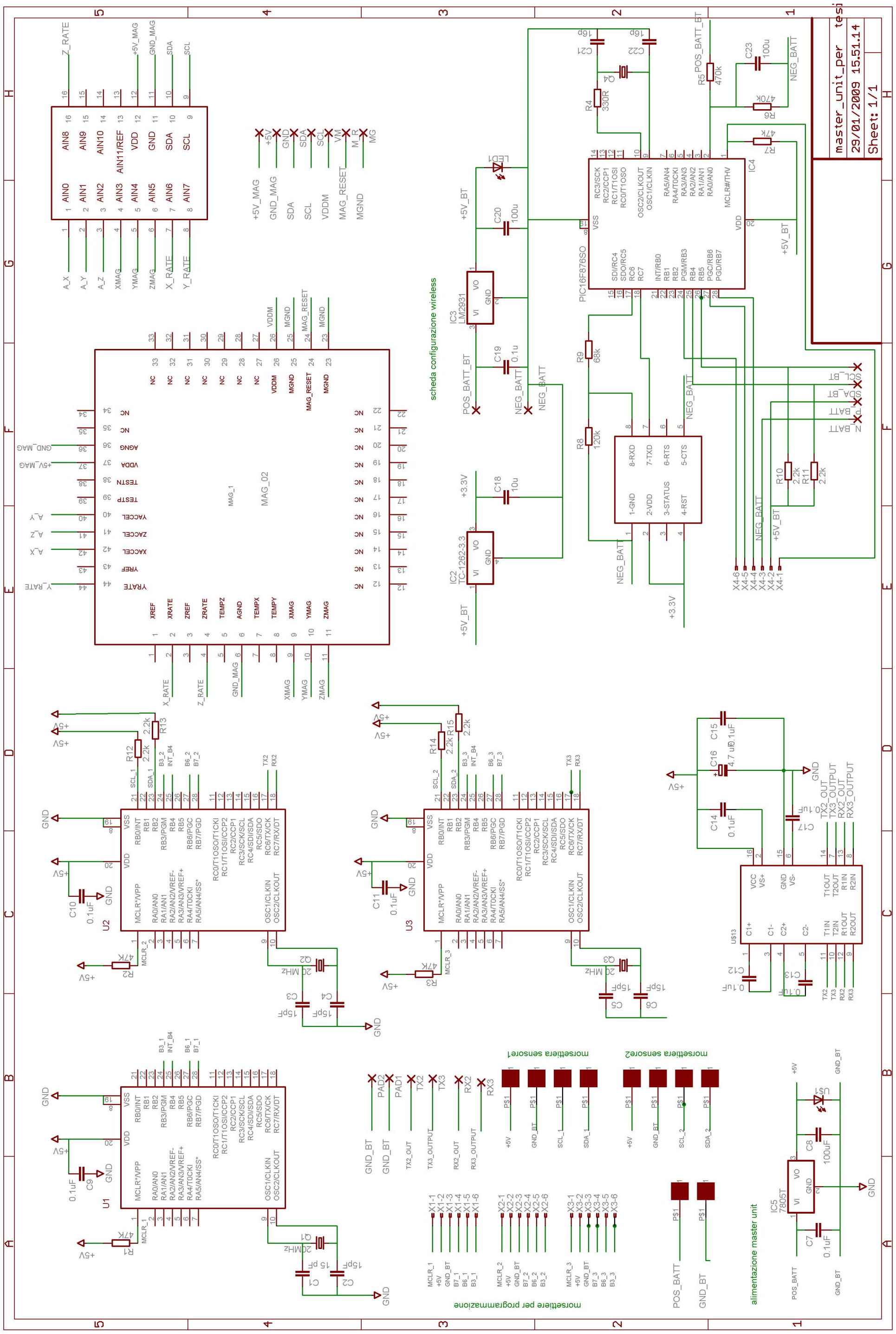
master_unit_per_tesi
29/01/2009 15.51.14
Sheet: 1/1
scheda configurazione wireless
PIC16F876SO
MAG_02
morsettiera sensore1
morsettiera sensore2
morsettiere per programmazione
alimentazione master unit

Appendix B

Calibration Procedure

The calibration procedure proposed is specifically designed in order to be executed from untrained personell and suitable for unstructured and ecological environments: it does not require any particular additional instruments, such as devices for accurate alignment, and it can be executed without modify environment conditions, for example without using additional knowing field. All it needs is a wooden box into which put the instrumented toys which have to be calibrated. The instrumented toy (of whatever shape) is secured inside a wooden box, shaped as a parallelepiped, so that the toy would not move as the box is displaced around. The box is placed on a wooden table and it is used as a reference frame for the turning movements the calibration procedure is composed by. Three overall movement sequences are needed: one for each kind of sensor.

Accelerometers The box is placed on the table on its A face (Fig. 1). After about two seconds (Waiting Time), it is smoothly (i.e. avoiding shocks) tilted by 90 deg (Fig. 2) along one edge, this is repeated four times until the box returns in the initial position doing an overall rotation of 360 deg (rotation 1). The whole procedure is repeated around a different horizontal axis (rotation 2)

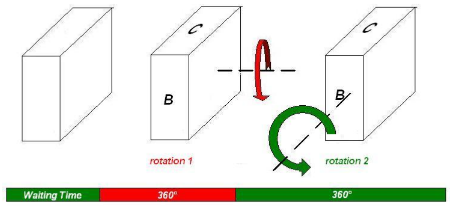

Figure B.1: Accelerometer calibration: movement sequence

Gyroscopes The box is placed on the table on its E face (Fig. 1). After about two seconds (Waiting Time), it is smoothly tilted by 90 deg (Fig. 3) along the edge between faces B, E in position II (with B face of the box parallel and in contact with the table). From position II the box is tilted by 90 deg along the edge between faces A, B in position III (with A face of the box parallel and in contact with the table). From position III the box is tilted by 90 deg along the edge between faces A, F in the final position (with F face of the box parallel and in contact with the table).

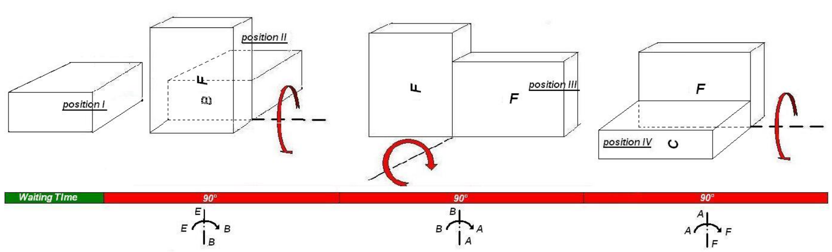

Figure B.2: Gyroscope calibration: movement sequence

Magnetometers The box is placed on the table on its B face (Fig. 1). After about two seconds (Waiting Time), an approximately 360 deg rotation (Fig. 4) is performed by keeping B face of the box always parallel and in contact with the table (rotation 1). The box is tilted by 90 deg (rotation 2) along one edge (highlighted in yellow) in position II. In this position a second approximately 360 deg rotation is performed on C face (rotation 3).

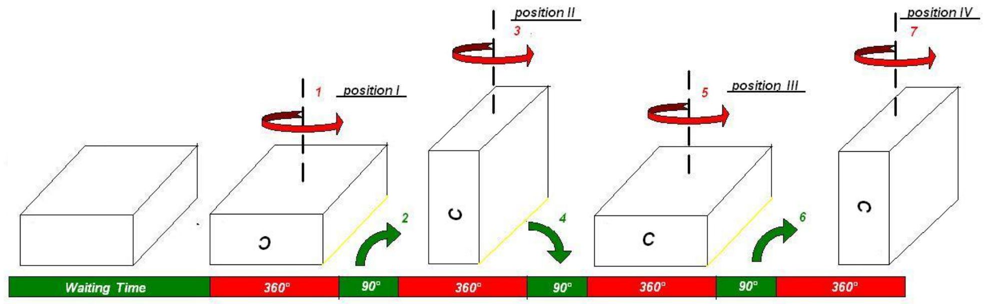

Figure B.3: Magnetometer calibration: movement sequence

This procedure is repeted until to arrive in position IV (D face parallel and in contact with the table).

Bibliography

[1] C. von Hofsten (2004), "An action perspective on motor development.", Trends Cogn Sci, 8:266-272.

[2] A. L. H. Van der Meer, F. R. Van der Weel, & D. N. Lee(1995), "The functional significance of arm movements in neonates.", Science, 267:693-695.

[3] R. Gerlai (2002), "Phenomics: fiction or the future?", Trends Neurosci, 25:506-509.

[4] J.D. Schmahmann (2004), "Disorders of the cerebellum: ataxia, dysmetria of thought, and the cerebellar cognitive affective syndrome.", J Neuropsychiatry Clin Neurosci, 16:367-378.

[5] A.M. Graybiel (1997), "The basal ganglia and cognitive pattern generators. Schizophr Bull.", Schizophrenia Bulletin, 23:459-469.

[6] F. Keller , A.M. Persico (2003), "The neurobiological context of autism.", Mol Neurobiol, 28:1-22.

[7] D.J. Grelotti, I. Gauthier, R.T. Schultz (2003), "Social interest and the development of cortical face specialization: what autism teaches us about face processing.", Dev Psychobiol, 40:213-225.

Fabrizio Taffoni

[8] E. Milne, J. Swettenham, P. Hansen, R. Campbell, H. Jeffries, K. Plaisted (2002), "High motion coherence thresholds in children with autism.", J Child Psychol Psychiatry, 43:255-263.

[9] J. Spencer, J. O'Brien, K. Riggs, O. Braddick, J. Atkinson, J. Wattam-Bell (2000), "Motion processing in autism: evidence for a dorsal stream deficiency.", Neuroreport, 11:2765-2767.

[10] A. Bertone, L. Mottron, P. Jelenic, J. Faubert (2003), "Motion perception in autism: a "complex" issue", J Cogn Neurosci, 15:218-225.

[11] Y. Takarae , N.J. Minshew , B. Luna , C.M. Krisky, J.A. Sweeney (2004), "Pursuit eye movement deficits in autism.", Brain, 127(12):2584-2594.

[12] R. Landry , S.E. Bryson (2004), "Impaired disengagement of attention in young children with autism (2004) J Child Psychol Psychiatry.", 45(6):1115-22.

[13] E. Courchesne, B.A. Kilman, R. Galambos, A.J. Lincoln (1984), "Autism: processing of novel auditory information assessed by event-related brain potentials.", Electroencephalogr Clin Neurophysiol, 59:238-248.

[14] N. Boddaert, N. Chabane, P. Belin, M. Bourgeois, V. Royer, C. Barthelemy, M.C. Mouren-Simeoni, A. Philippe, Brunelle F., Y. Samson, M. Zilbovicius (2004), "Perception of complex sounds in autism: abnormal auditory cortical processing in children.", Am. J. Psychiatry, 161:2117-2120.

[15] J. Swettenham, S. Baron-Cohen, T. Charman, A. Cox, G. Baird, A. Drew, L. Rees, S. Wheelwright (1998), "The frequency and distribution of spontaneous attention shifts between social and nonsocial stimuli in autistic, typically developing, and nonautistic developmentally delayed infants.", J. Child Psychol. Psychiatry, 39:747-753.

[16] S. Maestro, F. Muratori, M.C. Cavallaro, F. Pei, D. Stern, B. Golse, F. Palacio-Espasa (2002), "Attentional skills during the first 6 months of age in autism spectrum disorder.", J. Am. Acad. Child Adolesc. Psychiatry, 41:1239-1245.

[17] R.P. Hobson, M. Bishop (2003) "The pathogenesis of autism: insights from congenital blindness", Philos. Trans. R. Soc. Lond. B. Biol. Sci., 358:335-344.

[18] N.J. Minshew, K. Sung, B.L. Jones, J.M. Furman (2004), "Underdevelopment of the postural control system in autism.", Neurology, 63:2056-2061.

[19] C. Schmitz, J. Martineau, C. Barthelemy, C. Assaiante (2003), "Motor control and children with autism: deficit of anticipatory function?", Neurosci Lett, 348:17-20.

[20] C.A. Molloy, K.N. Dietrich , A. Bhattacharya (2003), "Postural stability in children with autism spectrum disorder." J. Autism Dev. Disord., 33:643-652.

[21] K. Pierce, E. Courchesne (2001), "Evidence for a cerebellar role in reduced exploration and stereotyped behavior in autism.", Biol Psychiatry 49:655-664.

[22] J.A. Sweeney, Y. Takarae, C. Macmillan, B. Luna, N.J. Minshew (2004), "Eye movements in neurodevelopmental disorders.", Curr Opin Neurol. 17:37-42.

[23] M. Hallett, M.K. Lebiedowska, S.L. Thomas, S.J. Stanhope, M.B. Denckla, J. Rumsey (1993), "Locomotion of autistic adults.", Arch Neurol 50:1304-1308.

[24] M.A. Dziuk, J.C. Gidley Larson, A. Apostu, E.M. Mahone, M.B. Denckla, S.H. Mostofsky (2007), "Dyspraxia in autism: association with

motor, social, and communicative deficits.", Dev. Med. Child. Neurol. 49(10):734-9.

[25] N.J. Rinehart, J.L. Bradshaw, A.V. Brereton, B.J. Tonge (2001), "Movement preparation in high-functioning autism and Asperger disorder: a serial choice reaction time task involving motor reprogramming.", J. Autism. Dev. Disord., 31:79-88.

[26] M. Mari, U. Castiello, D. Marks, C. Marraffa, M. Prior (2003), "The reach-to-grasp movement in children with autism spectrum disorder.", Philos. Trans. R. Soc. Lond. B. Biol. Sci., 358:393-403.

[27] P. Teitelbaum, O. Teitelbaum, J. Nye, J. Fryman and R.G. Maurer (1998), "Movement analysis in infancy may be useful for early diagnosis of autism.", Proc. Natl Acad Sci USA, 95: 13982.

[28] O. Teitelbaum, T. Benton, P.K. Shah, A. Prince, J.L. Kelly, P. Teitelbaum (2004), "Eshkol-Wachman movement notation in diagnosis: the early detection of Asperger's syndrome.", Proc Natl Acad Sci U S A, 101:11909-11914.

[29] M.K. Belmonte, G. Allen, A. Beckel-Mitchener, L.M. Boulanger, R.A. Carper, S. J. Webb (2004), "Autism and Abnormal Development of Brain Connectivity." J Neuroscience., 24(42):9228-9231.

[30] E. Courchesne, E. Redcay, J.T. Morgan, D.P. Kennedy (2005), "Autism at the beginning: microstructural and growth abnormalities underlying the cognitive and behavioral phenotype of autism.", Dev. Psychopathol. 17(3):577-97.

[31] B. Auyeung, S. Baron-Cohen, S. Wheelwright, C. Allison (2008), "The Autism Spectrum Quotient: Children's Version (AQ-Child).", J Autism Dev Disord. 38(7):1230-40.

[32] B. Robins, K. Dautenhahn, Te. Boekhorst, A. Billard (2005), “Robotic assistants in therapy and education of children with autism: can a small humanoid robot help encourage social interaction skills?” Univ Access Inf Soc. 4:105-120.

[33] B. Scassellati (2005), “How social robots will help us to diagnose, treat, and understand autism”, 12th International Symposium on Robotics Research (ISRR). San Francisco, CA.

[34] I.P. Werry, K. Dautenhahn, “Applying (1999) Mobile Robot Technology to the Rehabilitation of Autistic Children”, in Proceedings of SIRS 99, Symposium on Intelligent Robotics Systems.

[35] A. Billard, B. Robins, K. Dautenhahn, J. Nadel (2006) “Building Robota, a Mini-Humanoid Robot for the Rehabilitation of Children with Autism”. the RESNA Assistive Technology Journal.

[36] H. Kozima (2005), Interactive robots for communication-care: a case-study in autism therapy, 341-346, ROMAN.

[37] F. Michaud, C. Thberge-Turmel (2002) “Mobile robotic toys and autism”, Socially Intelligent Agents - Creating Relationships with Computers and Robots, Kerstin Dautenhahn, Alan Bond, Lola Canamero, Bruce Edmonds (editors), Kluwer Academic Publishers, pages 125-132.

[38] `http://paro.jp/english/index.html` (last accessed:19/07/2008)

[39] C. Trevarthen, S. Daniel (2005) “Disorganized rhythm and synchrony: Early signs of autism and Rett syndrome.”, Brain & Development 27: S25–S34

[40] D. Campolo, F. Taffoni, G. Schiavone, C. Laschi, F. Keller, E. Guglielmelli (2008) "Towards the Early Diagnosis of Neurodevelopmental Disorders: a Novel Technological Approach", procs of Int.Conf. on Technology and Applications in Biomedicine 2008 (ITAB08), 531-534.

[41] D. Campolo, F. Taffoni, G. Schiavone, C. Laschi, F. Keller, E. Guglielmelli (2008) "A Novel Technological Approach Towards the Early Diagnosis of Neurodevelopmental Disorders", procs of Int. Conf. on Engineering in Medicine and Biology Society 2008 (EMBC08), 4875-4878 .

[42] F. Taffoni, D. Campolo, E. Guglielmelli, F. Cecchi, S.M. Serio, C. Laschi, P. Dario (2008) "Sensorized ball for early diagnosis of neurodevelopmental disorders" in proc of Congresso Nazionale Bioingegneria.

[43] F. Taffoni, G. Schiavone, D. Campolo, F. Keller , E. Guglielmelli (2008) "Wearable Devices for infants behavioural analysis", in proc of Congresso Nazionale Bioingegneria.

[44] Martin J H, Engber D, Meng Z (2005), Effect of forelimb use on postnatal development of the forelimb motor representation in primary motor cortex of the cat. Journal of Neurophysiology, 93:2822.

[45] Martin J H, Choy M, Pullman S, Meng Z (2004), Corticospinal system development depends on motor experience. Journal of Neuroscience. 24:2122.

[46] J. J. Lockmann (2000), "A Perception-Action Perspective on Tool Use Development.", Child Development, 71(1):137-144.

[47] G. Welch, . Foxlin (2002), "Motion Tracking: No Silver Bullet, but a Respectable Arsenal.", IEEE Computer Graphics and Applications, 22(6): 24-38.

[48] B. Kemp, A.J.M.W. Janssen, B. van der Kamp (1998), "Body position can be monitored in 3D using miniature accelerometers and earth-magnetic field sensors", Electroencephalography and Clinical Neurophysiology, 109:484-488.

[49] D. Campolo, F. Keller, E. Guglielmelli (2006) "Inertial/Magnetic Sensors Based Orientation Tracking on the Group of Rigid Body Rotations with Application to Wearable Devices.",in procs of International Conference on Intelligent Robots and Systems 2006 IEEE/RSJ, 4762 - 4767.

[50] D. Campolo, M. Fabris, G. Cavallo, D. Accoto, F. Keller, E. Guglielmelli (2006), "A Novel Procedure for In-field Calibration of Sourceless Inertial/Magnetic Orientation Tracking Wearable Devices.", the first IEEE / RAS-EMBS Intl Conf. on Biomedical Robotics and Biomechatronics (BIOROB), Pisa, Italy.

[51] R. M. Murray, Z. Li, S. S. Sastry (1994), "A Mathematical Introduction to Robotic Manipulation", CRC Press 1994.

[52] C. Einspieler, H.F.R Prechtl (2005) "Prechtl's assessment of general Movements: a diagnostic tool for the functional assessment of the young nervous system.", Mental Retardation and Developmental Disabilities, 11:61-67.

[53] H.F.R. Prechtl, R.Nolte (1984) Motor behaviour of preterm infants. In: Prechtl HFR, editor. Continuity of neural functions from prenatal to postnatal life. Clin Dev Med 94. Oxford: Blackwell. p 79–92.

[54] Highway Safety Research Institute the university of Michigan Ann Arbor, Michigan 48109 (1978) "Antropometry of infants, children and youths to age 18 for product safety design".

[55] Schneider, K. and Zernicke, R. F. (1992) Mass, center of mass, and moment of inertia estimates for infant limb segments. J. Biomech. 25: 145-148.

[56] F. Taffoni, D. Campolo, J. Delafield-Butt, F. Keller, E. Guglielmelli, (2008) "Design and Assembling of a Magneto-Inertial Wearable Device

for Ecological Behavioral Analysis of Infants", in Proc. of IEEE/IROS Int. Conf. on Intelligent RObot System 2008, 3832-3837, Nice, France.

[57] H. Örnkloo & C. von Hofsten (2008),"Fitting objects into holes: On the development of spatial cognition skills" , Developmental Psychology, 2008, in press.

[58] F. Taffoni, D. Campolo, D. Formica,E. Guglielmelli, F. Cecchi, S.M. Serio, C. Laschi, P. Dario (2008) "Sensorized Toys for early diagnosis of neurodevelopmetal disorders" PAED 08.

[59] D. Kirsch (1996), " Adapting the Environment Instead of Oneself", Adaptive Behavior, 4(3-4): 415-452.

[60] JF. Babinski (1902), "Sur le role du cervelet dans les actes volitionnels necessitant une succession rapide de mouvements (diadococinese).", Rev Neurol 10:1013–1015.

[61] C. M. Freitag, C. Kleser, M. Schneider, A. von Gontard (2007) , "Quantitative Assessment of Neuromotor Function in Adolescents with High Functioning Autism and Asperger Syndrome", J. Autism Dev Disord 37:948–959.

[62] R.C. Oldfield (1971), "The assessment and analysis of handedness: The Edinburgh inventory.", Neuropsychologia, 9, 97-113.

[63] M. D. Mauk and D. V. Buonomano (2004), "The Neural Basis of Temporal Processing",Annu Rev Neurosci 27:307-340

[64] G. Koch, M. Oliveri, S. Torriero, · S. Salerno, E. Lo Gerfo, C. Caltagironeat (2007) , Repetitive TMS of cerebellum interferes with millisecond time processing, Exp Brain Res. 179:291-299

[65] M. F. Del Olmo, B, Cheeran, G, Koch and J, C. Rothwell (2007), "Role of the Cerebellum in Externally Paced Rhythmic Finger Movements", J Neurophysiol 98:145-152